Inorganic Chemistry
Article

Inorg. Chem. **2009**, *48*, 9191–9204 **9191**
DOI: 10.1021/ic900691a

Homo- and Heterometallic Complexes of Tetra-(Di-Substituted Hydroxybenzyl)-*N,N′*-Ethylenediamine Derivatives

Timothy J. Boyle,* Harry D. Pratt, III, Leigh Anna M. Ottley, Todd M. Alam, Sarah K. McIntyre, and Mark A. Rodriguez

Advanced Materials Laboratory, Sandia National Laboratories, 1001 University Boulevard, SE, Albuquerque, New Mexico 87106

Joshua Farrell

Department of Chemistry, College of the Holy Cross, Box C, 1 College Street, Worcester, Massachusetts 01610

Charles F. Campana

Bruker AXS Inc., 5465 East Cheryl Parkway, Madison, Wisconsin 53711-5373

Received April 8, 2009

The coordination behavior of a series of group 4 metal alkoxides [$M(OR)_4$] modified by a set of novel substituted hydroxybenzyl ethylene diamine (H_4-ED-L_4) ligands {[tetra(3,5-di-*t*-butyl-2-hydroxybenzyl)-*N,N′*-ethylenediamine] termed H_4-ED-DBP_4 (**1**), [tetra(3,5-di-*t*-amyl-2-hydroxybenzyl)-*N,N′*-ethylenediamine] termed H_4-ED-DAP_4 (**1a**), and [tetra(3,5-dichloro-2-hydroxybenzyl)-*N,N′*-ethylenediamine] termed H_4-ED-DCP_4 (**2**)} was elucidated. The reaction of **1** or **1a** with the $M(OR)_4$ precursor led to the isolation of the structural similar species M(ED-L_4) where L = DBP, M=Ti (**3**), Zr (**4**), Hf (**5**); L = DAP, M = Zr (**4a**), Hf (**5a**). In contrast, the reaction of **2** with the $M(OR)_4$ precursors yielded Ti(ED-DCP_4) (**6**), $(py)_2$Zr(ED-DCP_4) (**7**), and ($HOBu^t$)Hf(ED-DCP_4) (**8**) where py = pyridine and $HOBu^t$ = $HOC(CH_3)_3$. For **3**−**6**, the cations of the monomeric species were completely encapsulated by all available heteroatoms (four O and two N) of the ED-L_4 ligands, yielding an octahedral geometry for each metal center. For **7** and **8**, an identical binding by the ED-DCP_4 ligand was observed with the additional coordination of Lewis basic adducts, forming 8- and 7-coordinated metal centers, respectively. Switching to +2 cations led to the isolation of $[(THF)Ca]_2$(ED-DBP_4) (**9a**) where THF=tetrahydrofuran, $\{[(py)Ca]_4$(ED-(μ-DBP-η^6)$_4$)$_2\}_n$ (**9b**), and [(py)Zn](ED-DBP_4)[$Zn(py)_2$] (**10**) •5py and $[(py)Sn]_2$(ED-DBP_4) (**11**). The structures of these species were significantly different in arrangement compared to the Group 4 derivatives. Further attempts to produce a mixed +4/+2 cationic species yielded [(py)$(ONep)_2$Ti(ED-DBP_4)Zn(py)] (**12**). Reacting the single-source precursor Co[μ-$OC_6H_4(CHMe_2)_2$-2)$_2$Li-$(py)_2]_2$ with **1**, led to the isolation of (py)Li[ED-DBP_3(H-DBP)]Co (**13**), with one of the phenol protons remaining unreacted. The synthesis and characterization of these compounds are presented in detail.

Introduction

The physical properties of metal alkoxides ($M(OR)_x$) such their as high solubility, high volatility, and low thermal decomposition temperatures have made them ideal precursors for sol−gel, metalorganic chemical vapor deposition, and nanoparticle processes.[1−31] Often overlooked, however, is the role that the structure of the precursor plays in influencing the properties of the ceramic oxide produced. The close connection between the $M(OR)_x$ structure and the final material's characteristics (i.e., density, morphology, processing temperature, etc.) has been clearly demonstrated for a number of systems.[1−20] Therefore, if ceramic materials are to

*To whom correspondence should be addressed. E-mail: tjboyle@sandia.gov. Phone: (505)272-7625. Fax: (505)272-7336.

(1) Bell, N. S.; Tallant, D. R.; Raymond, R.; Boyle, T. J. *J. Mater. Res.* **2008**, *23*, 529.
(2) Hernandez-Sanchez, B. A.; Boyle, T. J.; Baros, C. M.; Brewer, L. N.; Headley, T. J.; Tallant, D. R.; Rodriguez, M. A.; Tuttle, B. A. *Chem. Mater.* **2007**, *19*, 1459.
(3) Boyle, T. J.; Sewell, R. M.; Ottley, L. A. M.; Pratt, H. D.; Quintana, C. J.; Bunge, S. D. *Inorg. Chem.* **2007**, *46*, 1825.
(4) Boyle, T. J.; Ottley, L. A. M.; Daniel-Taylor, S. D.; Tribby, L. J.; Bunge, S. D.; Costello, A. L.; Alam, T. M.; Gordon, J. C.; McCleskey, T. M. *Inorg. Chem.* **2007**, *46*, 3705.
(5) Gerung, H.; Boyle, T. J.; Tribby, L. J.; Bunge, S. D.; Brinker, C. J.; Han, S. M. *J. Am. Chem. Soc.* **2006**, *128*, 5244.

Published on Web 09/11/2009

be rationally developed using M(OR)x, it is critical that their structure be fully understood. Unfortunately, structural elucidation for $M(OR)_x$ a priori is difficult because of the large ratio of cation size to ligand charge. This variation often leaves open coordination sites on the metal centers, which can be filled through the use of bridging alkoxide (μ-OR) ligands leading to uncontrolled clusters, oligomers, or polymers.[27−31] Hence, any hope of making tailored ceramic materials from $M(OR)_x$ requires garnering control over their structure.

In a number of $M(OR)_x$ systems, multidentate ligands have been found to lend some control over the final structures isolated. For instance, using select polydentate ligands that employ heteroatoms in the pendant chains or rings, such as 4,6-dihydroxypyrimidine (H_2-DHP),[32] pyridine carbinol (H-OPy),[3,33] 2-mercaptopyridine *n*-oxide (H-2MPO),[34] and 3,3′-dihydroxy 2,2′-bipyridine (H_2-OBPy)[34] (shown in Figure 1) controlled assemblies have been realized. From this set of ligands, the nitrogen bearing DHP and OBPy ligands were found to act solely as bridging moieties for $Ti(OR)_4$ derivatives. In contrast, the OPy [3,33] and 2MPO[34] ligands were reported to bind in a bidentate chelating manner for a series of $Ti(OR)_4$, thereby allowing for select chemical manipulations on the opposite side of the cation.

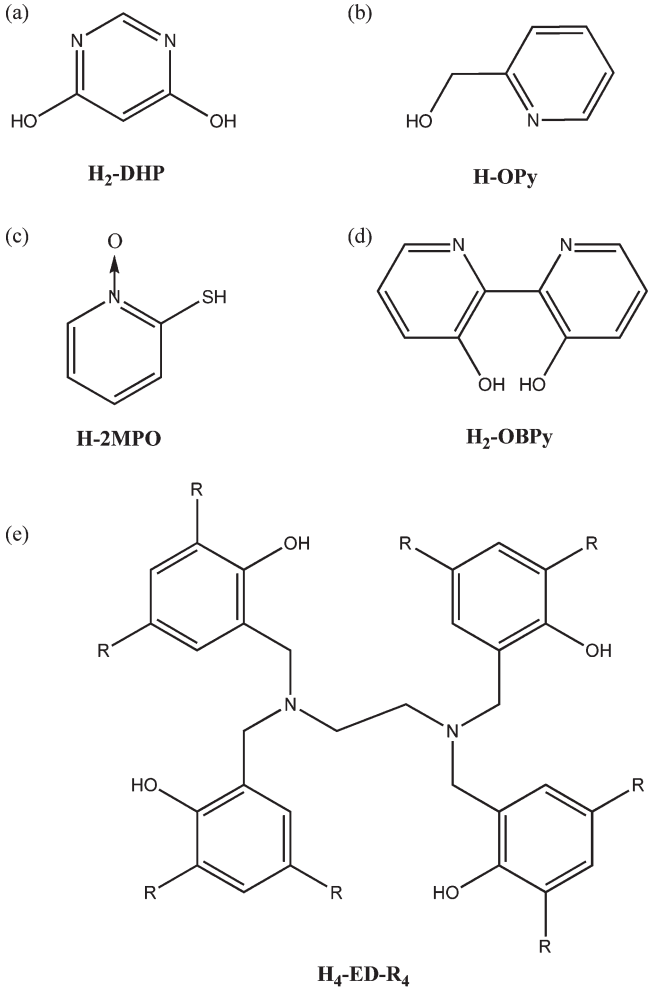

Figure 1. Schematic of ligands investigated (a) dihydroxypyridimine (H_2-DHP), (b) pyridine carbinol (H-OPy), (c) mercapto pyridine *n*-oxide (H-2MPO), (d) 3,3′-dihydroxy 2,2′-bipyridine (H_2-OBPy), (e) tetrakis (2,4-disubstituted phenol) ethylenediamine (R = *t*-butyl or H_4-ED-DBP_4 (**1**)), R = amyl or H_4ED-DAP_4 (**1a**)), and (R = Cl or H_4-ED-DCP_4 (**2**).

Since these heteroatom-containing, alkoxide ligands have successfully introduced some structural control over the final $M(OR)_x$, investigation into other, more complex heteroatom bearing ligands were of interest. For this study, tetrakis-(3,5-alkyl substituted 2-hydroxy)-*N*,*N*′-ethylene diamine ligated compounds (H_4-ED-L_4, Figure 1e)[35] were thought to be promising based on their multidentate nature and high solubility in organic solvents. The ligands studied here include [tetra(3,5-di-*t*-butyl-2-hydroxybenzyl)-*N*,*N*′-ethylenediamine] termed H_4-ED-DBP_4 (**1**), [tetra(3,5-di-*t*-amyl-2-hydroxybenzyl)-*N*,*N*′-ethylenediamine] termed H_4-ED-DAP_4 (**1a**), and [tetra(3,5-dichloro-2-hydroxybenzyl)-*N*,*N*′-ethylenediamine] termed H_4-ED-DCP_4 (**2**) derivatives. A schematic of these compounds is shown in Figure 1e.

(6) Boyle, T. J.; Ottley, L. A. M.; Rodriguez, M. A. *Polyhedron* **2005**, *24*, 1727.
(7) Boyle, T. J.; Bunge, S. D.; Clem, P. G.; Richardson, J.; Dawley, J. T.; Ottley, L. A. M.; Rodriguez, M. A.; Tuttle, B. A.; Avilucea, G. R.; Tissot, R. G. *Inorg. Chem.* **2005**, *44*, 1588.
(8) Boyle, T. J.; Bunge, S. D.; Alam, T. M.; Holland, G. P.; Headley, T. J.; Avilucea, G. *Inorg. Chem.* **2005**, *44*, 1309.
(9) Coker, E. N.; Boyle, T. J.; Rodriguez, M. A.; Alam, T. M. *Polyhedron* **2004**, *23*, 1739.
(10) Boyle, T. J.; Bunge, S. D.; Andrews, N. L.; Matzen, L. E.; Sieg, K.; Rodriguez, M. A.; Headley, T. J. *Chem. Mater.* **2004**, *16*, 3279.
(11) Boyle, T. J.; Ward, T. L.; De'Angeli, S. M.; Xu, H. F.; Hammetter, W. F. *Chem. Mater.* **2003**, *15*, 765.
(12) Boyle, T. J.; Rodriguez, M. A.; Ingersoll, D.; Headley, T. J.; Bunge, S. D.; Pedrotty, D. M.; De'Angeli, S. M.; Vick, S. C.; Fan, H. Y. *Chem. Mater.* **2003**, *15*, 3903.
(13) Boyle, T. J.; Coker, E. N.; Zechmann, C. A.; Voigt, J. A.; Rodriguez, M. A.; Kemp, R. A. *Chem. Mater.* **2003**, *15*, 309.
(14) Boyle, T. J.; Alam, T. M.; Rodriguez, M. A.; Zechmann, C. A. *Inorg. Chem.* **2002**, *41*, 2574.
(15) Zechmann, C. A.; Boyle, T. J.; Rodriguez, M. A.; Kemp, R. A. *Polyhedron* **2000**, *19*, 2557.
(16) Gallegos, J. J.; Ward, T. L.; Boyle, T. J.; Rodriguez, M. A.; Francisco, L. P. *Chem. Vap. Deposition* **2000**, *6*, 21.
(17) Boyle, T. J.; Alam, T. M.; Tafoya, C. J.; Scott, B. L. *Inorg. Chem.* **1998**, *37*, 5588.
(18) Boyle, T. J.; Alam, T. M.; Mechenbier, E. R.; Scott, B. L.; Ziller, J. W. *Inorg. Chem.* **1997**, *36*, 3293.
(19) Boyle, T. J.; Schwartz, R. W.; Doedens, R. J.; Ziller, J. W. *Inorg. Chem.* **1995**, *34*, 1110.
(20) Boyle, T. J.; Schwartz, R. W. *Comm. Inorg. Chem.* **1994**, *16*, 243.
(21) Boyle, T. J.; Pratt, H. D.; Alam, T. M.; Rodriguez, M. A.; Clem, P. G. *Polyhedron* **2007**, *26*, 5095.
(22) Boyle, T. J.; Ottley, L. A. M.; Brewer, L. N.; Sigman, J.; Clem, P. G.; Richardson, J. J. *Eur. J. Inorg. Chem.* **2007**, 3805.
(23) Boyle, T. J.; Hernandez-Sanchez, B. A.; Baros, C. M.; Brewer, L. N.; Rodriguez, M. A. *Chem. Mater.* **2007**, *19*, 2016.
(24) Boyle, T. J.; Tribby, L. J.; Bunge, S. D. *Eur. J. Inorg. Chem.* **2006**, 4553.
(25) Gerung, H.; Bunge, S. D.; Boyle, T. J.; Brinker, C. J.; Han, S. M. *Chem. Commun.* **2005**, *14*, 1914.
(26) Boyle, T. J.; Tribby, L. J.; Alam, T. M.; Bunge, S. D.; Holland, G. P. *Polyhedron* **2005**, *24*, 1143.
(27) Bradley, D. C. *Chem. Rev.* **1989**, *89*, 1317.
(28) Bradley, D. C.; Mehrotra, R. C.; Gaur, D. P. *Metal Alkoxides*; Academic Press: New York, 1978.
(29) Caulton, K. G.; Hubert-Pfalzgraf, L. G. *Chem. Rev.* **1990**, *90*, 969.
(30) Chandler, C. D.; Roger, C.; Hampden-Smith, M. *J. Chem. Rev.* **1993**, *93*, 1205.
(31) Hubert-Pfalzgraf, L. G. *New J. Chem.* **1987**, *11*, 663.
(32) Boyle, T. J.; Rodriguez, M. A.; Alam, T. M. *Dalton Trans.* **2003**, 4598.
(33) Boyle, T. J.; Ottley, L. A. M.; Rodriguez, M. A.; Sewell, R. M.; Alam, T. M.; McIntyre, S. K. *Inorg. Chem.* **2008**, *47*, 10708.
(34) Boyle, T. J.; Ottley, L. A. M.; Rodriguez, M. A. *Polyhedron* **2008**, *27*, 3079.
(35) Higham, C. S.; Dowling, D. P.; Shaw, J. L.; Cetin, A.; Ziegler, C. J.; Farrell, J. R. *Tetrahedron Lett.* **2006**, *47*, 4419.

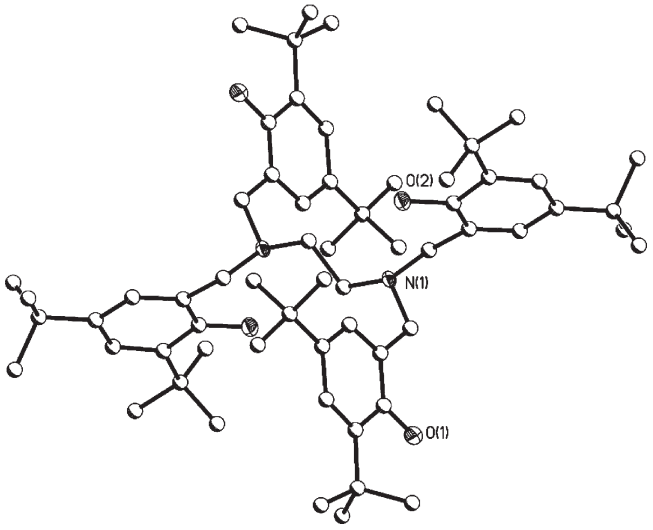

Figure 2. Structure plot of **1**. Heavy atom thermal ellipsoids drawn at 30% level, and carbon atoms drawn as ball and stick for simplicity. Py molecules omitted for clarity.

Because of the lack of structurally characterized species in the literature and the interesting polychelating effect observed for similar literature compounds,[35−38] it was decided to explore the coordination behavior of these H_4-ED-L_4 ligands with the group 4 $M(OR)_4$ congeners. The initial 1:1 stoichiometry successfully generated a novel family of ED-L_4 chelated species identified as M(ED-DBP_4) M = Ti (**3**), Zr (**4**), Hf (**5**), M(ED-DAP_4) M = Zr (**4a**), Hf (**5a**), and Ti(ED-DCP_4) (**6**), $(py)_2$Zr(ED-DCP_4) (**7**), and ($HOBu^t$)Hf(ED-DCP_4) (**8**) where py = pyridine and $HOBu^t = HOC(CH_3)_3$. In addition, the homometallic $[(THF)Ca]_2$(ED-DBP_4) (**9a**) where THF = tetrahydrofuran, $\{[(py)Ca]_4$(ED-(μ-DBP-η^6)$_4)_2\}_n$ (**9b**), [(py)Zn](ED-DBP_4)[Zn(py)$_2$] (**10**) •5py, and $[(py)Sn]_2$(ED-DBP_4) (**11**) as well as the heterometallic [(py)$(ONep)_2$-Ti(ED-DBP_4)Zn(py)] (**12**) where ONep = $OCH_2C(CH_3)_3$, and (py)Li[ED-$(DBP)_3$(H-DBP)]Co (**13**) have been isolated. The synthesis and structural characterization of these compounds are reported in detail below.

Experimental Section

Organic Ligand. The H_4-ED-L_4 ligands (**1**, **1a**, and **2**) were prepared through slight modification of literature procedures.[35] The full description for **1a** is supplied, since it has not been previously disseminated. The following chemicals were used as received (Aldrich): 3, 5-di-*t*-amyl phenol (H-DAP), ethylene diamine (ED-H4) and paraformaldehyde (H- PF).

H_4-ED-DAP_4 (1a). H-DAP (5.27 g, 22.5 mmol), ED-H_4 (0.225 g, 3.75 mmol), and H-PF (0.450 g, 15.0 mmol) heated, without solvent at 80 °C for 3 days.[35] Yield: 1.66 g (42.3%). FTIR (KBr, cm^{-1}): 3317, 2963, 2932, 2875, 2856, 1603 cm^{-1}. ^{1}H NMR (400 MHz, $CDCl_3$) δ 10.73 (b, 2H, DAP-O*H*), 7.09 (d, 2H, DAP-O*H*, J_{H-H} = 2.2 Hz), 6.79 (d, 2H, DAP-O*H*, J_{H-H} = 2.2 Hz), 3.97 (s, 4H, DAP-CH_2-N), 2.86 (s, 4H, N−CH_2-CH_2-N), 1.88 (q, 4H, $C(CH_3)_2$-CH_2-CH_3, J_{H-H} = 7.6 Hz), 1.58 (q, 4H, $C(CH_3)_2$-CH_2-CH_3, J_{H-H} = 7.6 Hz), 1.37 (s, 12H, $C(CH_3)_2$-CH_2−CH_3), 1.25 (s, 12H, $C(CH_3)_2$-CH_2−CH_3), 0.68 (t, 6H, $C(CH_3)_2$-CH_2−CH_3, J_{H-H} = 7.6 Hz), 0.66 (t, 6H, $C(CH_3)_2$-CH_2−CH_3, J_{H-H} = 7.6 Hz). ^{13}C NMR (100 MHz, $CDCl_3$) δ 154.4, 138.9, 134.4, 125.3, 124.0, 121.6, 53.7, 48.1, 38.6, 37.4, 37.3, 33.2, 28.8, 27.8, 9.8, 9.4. Mp 121−123 °C.

Inorganic Characterization. All compounds and reactions described were handled with rigorous exclusion of air and water using standard Schlenk line and argon filled glovebox techniques. All solvents were stored under argon and used as received in (Aldrich) Sure/SealTM bottles, including toluene (tol), tetrahydrofuran (THF), and pyridine (py). The following chemicals were used as received (Aldrich and Alfa Aesar): $Ti(OCH(CH_3)_2)_4$ ($Ti(OPr^i)_4$), $Zr(OC(CH_3)_3)_4$, ($Zr(OBu^t)_4$), 1.0 M $Zn(CH_2CH_3)_2$ in hexanes ($Zn(Et)_2$), $Hf(OC(CH_3)_3)_4$ ($Hf(OBu^t)_4$), and H−$OCH_2C(CH_3)_3$ (H-ONep). [Ti(μ-ONep)$(ONep)_3]_2$,[18] $Ca(NR_2)_2$[23] where R = $SiMe_3$, Co[μ-$OC_6H_4(CHMe_2)_2$-2)$_2$Li(py)$_2]_2$,[12] and $Sn(NMe_2)_2$[14] were prepared according to literature procedures.

FTIR data were obtained for KBr pressed pellets using a Bruker Vector 22 Instrument under an atmosphere of flowing nitrogen. Elemental analyses were performed on a Perkin-Elmer 2400 CHN-S/O Elemental Analyzer. All NMR samples were prepared from dried crystalline materials that were handled and stored under an argon atmosphere and redissolved in cyclohexane-d_{12} (cyclo-d_{12}), chloroform-*d* ($CDCl_3$) or pyridine-d_5 (py-d_5). All NMR spectra were obtained on a Bruker DRX 400 under standard experimental conditions. The ^{1}H and ^{13}C chemical shifts were referenced to the observed solvent resonances. Melting point determinations were made on sealed samples using an Electrotherm Melting Point Apparatus. Powder X-ray Diffraction (PXRD) patterns were collected on a PANalytical powder diffractometer with Cu Kα radiation (1.5406 Å) and a RTMS X'Celerator detector. Samples were scanned at a rate of 0.02°/2 s in the 2θ range of 10−100°. Dried crystalline powders were mounted directly onto a zero background holder. Mass spectroscopy (ESI) was obtained from University of Massachusetts Amherst, Mass Spectrometry Center (B-162 Conte Center, 120 Governors Drive, Amherst, MA −01003) using a JEOL MStation JMS700 high resolution two-sector spectrometer.

General Synthesis. Because of the similarity of synthesis of **3**−**8**, a general description is presented here with specific details listed for the respective compounds. The desired H_4-ED-L_4 was slowly added to a stirring solution of the appropriate $M(OR)_4$ dissolved in tol (~5 mL). Upon addition of the H_4-ED-L_4 ligand, the clear solutions turned a variety of colors ranging from pale yellow to bright orange dependent on both the metal and the ligand of interest. After 1 h, if a precipitate was present, the reaction was warmed slightly until it dissolved and then set aside to slowly cool. The unheated reactions were allowed to stir for 12h and then set aside to allow crystals to grow by slow evaporation of the volatile components of the reaction mixture. If crystals did not form, the sample was redissolved in tol and small amounts of py were added to facilitate crystallization. Yields were not optimized. *Note:* A majority of the elemental analyses were not found to be representative of the single crystal structure but are included here for completeness and possible reasons discussed in the text.

Ti(ED-DBP_4) (3). Used $Ti(OPr^i)_4$ (0.152 g, 0.536 mmol) and H_4-ED-DBP_4 (0.500 g, 0.536 mmol). Crystalline Yield: 0.258 g (49.4%). FTIR (KBr, cm^{-1}): 2957(s), 2868(m), 1600(m), 1465(s), 1413(w,sh), 1363(m), 1263(s), 1204(w), 1170(m), 1130(m), 1020(m), 856(s), 808(w), 761(m), 583(m), 551(m), 468(m). ^{1}H NMR (400.1 MHz, cyclo-d_{12}, * denotes free ligand resonances: δ 7.22 (1.3H, s, $[(CH_2N)(CH_2C_6H_2(O)$-2$(C(CH_3)_3)_2$-3,5$))_2]_2$), 7.12*−6.99*(1.1H, mult, $[(CH_2N)(CH_2C_6H_2(OH)$-2$(C(CH_3)_3)_2$-3,5$))_2]_2$), 7.16 (1.0H, s, $[(CH_2N)(CH_2C_6H_2(O)$-2$(C(CH_3)_3)_2$-3,5$))_2]_2$), 6.79 (1.0H, s, $[(CH_2N)(CH_2C_6H_2(O)$-2$(C(CH_3)_3)_2$-3,5$))_2]_2$), 6.75(1.3H, s, $[(CH_2N)(CH_2C_6H_2(O)$-2$(C(CH_3)_3)_2$-3,5$))_2]_2$), 4.43 (1.0H, d, $[(CH_2N)(CH_2C_6H_2(O)$-2$(C(CH_3)_3)_2$-3,5$))_2]_2$, J_{H-H} = 6.4 Hz), 4.08 (1.0H, d, $[(CH_2N)(CH_2C_6H_2(O)$-2$(C(CH_3)_3)_2$-3,5$))_2]_2$, J_{H-H} = 6.6 Hz), 3.47*(0.8H, s, $[(CH_2N)(CH_2C_6H_2(OH)$-2$(C(CH_3)_3)_2$-3,5$))_2]_2$),

(36) Vencato, I.; Neves, A.; Vincent, B. R.; Erasmus-Buhr, C.; Haase, W. *Acta Crystallogr., Sect C.: Cryst. Struct. Commun.* **1994**, *50*, 386.
(37) Neves, A.; Ceccato, A. S.; Vencato, I.; Mascarenhas, Y. P.; Erasmus-Buhr, C. *Chem. Commun.* **1992**, 652.
(38) Hefele, H.; Ludwig, E.; Bansse, W.; Uhlemann, E.; Lugger, T.; Hahn, E.; Mehner, H. *Z. Anorg. Allg. Chem.* **1995**, *621*, 671.

3.13 (1.0H, d, $[(CH_2N)(CH_2C_6H_2(O)\text{-}2(C(CH_3)_3)_2\text{-}3,5))_2]_2$, J_{H-H} = 6.6 Hz), 3.08 (0.9H, d, $[(CH_2N)(CH_2C_6H_2(O)\text{-}2(C(CH_3)_3)_2\text{-}3,5))_2]_2$, J_{H-H} = 4.3 Hz), 2.84 (1.0H, d, $[(CH_2N)(CH_2C_6H_2(O)\text{-}2(C(CH_3)_3)_2\text{-}3,5))_2]_2$, J_{H-H} = 6.7 Hz), 2.68* (0.4H, s, $[(CH_2N)(CH_2C_6H_2(OH)\text{-}2(C(CH_3)_3)_2\text{-}3,5))_2]_2$), 2.45 (1.0H, d, $[(CH_2N)(CH_2C_6H_2(O)\text{-}2(C(CH_3)_3)_2\text{-}3,5))_2]_2$, J_{H-H} = 4.3 Hz), 2.27* (1.0H, s, $[(CH_2N)(CH_2C_6H_2(OH)\text{-}2(C(CH_3)_3)_2\text{-}3,5))_2]_2$), 1.54 (9.2H, s, $[(CH_2N)(CH_2C_6H_2(O)\text{-}2(C(CH_3)_3)_2\text{-}3,5))_2]_2$), 1.33*, 1.24, 1.23* 1.21, 1.12 (41.7H, s, $[(CH_2N)(CH_2C_6H_2(O)\text{-}2(C(CH_3)_3)_2\text{-}3,5))_2]_2$). Anal. Calcd for $C_{62}H_{92}N_2O_4Ti$ (MW = 977.28): C, 76.20; H, 9.48; N, 2.87. Found: C, 76.31; H, 9.01; N, 2.65. MS(ESI+) *m/z*: $[M+H]^+$ calcd for $C_{62}H_{93}N_2O_4Ti$ (MW = 977.7). Found: 977.7, 933.8 (free ligand). Mp: 324 °C.

Zr(ED-DBP$_4$) (4). Used $Zr(OBu^t)_4$ (0.206 g, 0.536 mmol) and H_4-ED-DBP$_4$ (0.500 g, 0.536 mmol). Crystalline Yield: 0.199 g (36.3%). FTIR (KBr, cm^{-1}): 2957(s), 2928(s, sh), 2867(m), 1605(m), 1471(s), 1413(w), 1361(w), 1300(m,sh), 1265(s), 1169(w), 1130(m), 1096(m,br), 1030(m, br), 873(w), 846(s), 807(m), 752(m), 555(m), 466(m). ^{1}H NMR (400.1 MHz, cyclo-d_{12}): δ 7.24, 7.20 (2.1H, s, $[(CH_2N)(CH_2C_6H_2(O)\text{-}2(C(CH_3)_3)_2\text{-}3,5))_2]_2$), 6.79 (2.0H, s, $[(CH_2N)(CH_2C_6H_2(O)\text{-}2(C(CH_3)_3)_2\text{-}3,5))_2]_2$), 4.33 (1.0H, d, $[(CH_2N)(CH_2C_6H_2(O)\text{-}2(C(CH_3)_3)_2\text{-}3,5))_2]_2$, J_{H-H} = 6.5 Hz), 4.08 (1.0H, d, $[(CH_2N)(CH_2C_6H_2(O)\text{-}2(C(CH_3)_3)_2\text{-}3,5))_2]_2$, J_{H-H} = 6.6 Hz), 3.02 (1.1H, d, $[(CH_2N)(CH_2C_6H_2(O)\text{-}2(C(CH_3)_3)_2\text{-}3,5))_2]_2$, J_{H-H} = 6.6 Hz), 2.94 (1.0H, d, $[(CH_2N)(CH_2C_6H_2(O)\text{-}2(C(CH_3)_3)_2\text{-}3,5))_2]_2$, J_{H-H} = 4.5 Hz), 2.73 (1.0H, d, $[(CH_2N)(CH_2C_6H_2(O)\text{-}2(C(CH_3)_3)_2\text{-}3,5))_2]_2$, J_{H-H} = 6.6 Hz), 2.40 (1.0H, d, $[(CH_2N)(CH_2C_6H_2(O)\text{-}2(C(CH_3)_3)_2\text{-}3,5))_2]_2$, J_{H-H} = 4.5 Hz), 1.52 (9.1H, s, $[(CH_2N)(CH_2C_6H_2(O)\text{-}2(C(CH_3)_3)_2\text{-}3,5))_2]_2$), 1.24, 1.22, 1.17 (27.9H, s, $[(CH_2N)(CH_2C_6H_2(O)\text{-}2(C(CH_3)_3)_2\text{-}3,5))_2]_2$); see Supporting Information for spectrum. Anal. Calcd for $C_{62}H_{92}N_2O_4Zr$ (MW = 1020.60): C, 72.96; H, 9.08; N, 2.75. Found: C, 72.85; H, 8.88; N, 2.67. MS(ESI+) *m/z*: $[M+H]^+$ calcd for $C_{62}H_{93}N_2O_4Zr$ (MW = 1019.6) Found: 1019.7 Mp: > 360 °C.

Zr(ED-DAP$_4$) (4a). Used $Zr(OBu^t)_4$ (0.183 g, 0.478 mmol) and H_4-ED-DAP$_4$ (0.500 g, 0.478 mmol). Crystalline Yield: 0.147 g (27.3%). FTIR (KBr, cm^{-1}): 2963(s), 2913(s,sh), 2873(s), 1600(m), 1466(s), 1412(m), 1379(m), 1328(m), 1269(s), 1215(m), 1162(m), 1129(m), 1023(m), 873(s) 840(s), 793(m), 735(s), 542(s), 476(s,sh), 459(s). ^{1}H NMR (400.1 MHz, cyclo-d_{12}): δ 7.17, 7.11 (2.1H, s, $[(CH_2N)(CH_2C_6H_2(O)\text{-}2((C(CH_3)_2((CH_2CH_3))\text{-}3,5))_2]_2$), 6.72, 6.71(2.1H, s, $[(CH_2N)(CH_2C_6H_2(O)\text{-}2((C(CH_3)_2((CH_2CH_3))\text{-}3,5))_2]_2$), 4.31 (1.0H, d, $[(CH_2N)(CH_2C_6H_2(O)\text{-}2((C(CH_3)_2((CH_2CH_3))\text{-}3,5))_2]_2$, J_{H-H} = 6.6 Hz), 4.14 (1.0H, d, $[(CH_2N)(CH_2C_6H_2(O)\text{-}2((C(CH_3)_2((CH_2CH_3))\text{-}3,5))_2]_2$, J_{H-H} = 6.6 Hz), 3.03 (1.0H, d, $[(CH_2N)(CH_2C_6H_2(O)\text{-}2((C(CH_3)_2((CH_2CH_3))\text{-}3,5))_2]_2$, J_{H-H} = 6.6 Hz), 2.86 (1.0H, d, $[(CH_2N)(CH_2C_6H_2(O)\text{-}2((C(CH_3)_2((CH_2CH_3))\text{-}3,5))_2]_2$, J_{H-H} = 4.3 Hz), 2.74 (1.0H, d, $[(CH_2N)(CH_2C_6H_2(O)\text{-}2((C(CH_3)_2((CH_2CH_3))\text{-}3,5))_2]_2$, J_{H-H} = 6.6 Hz), 2.45 (1.0H, d, $[(CH_2N)(CH_2C_6H_2(O)\text{-}2((C(CH_3)_2((CH_2CH_3))\text{-}3,5))_2]_2$, J_{H-H} = 4.4 Hz), 2.27(5H, q, $[(CH_2N)(CH_2C_6H_2(O)\text{-}2((C(CH_3)_2((CH_2CH_3))\text{-}3,5))_2]_2$), 2.00 (1.0H, q, $[(CH_2N)(CH_2C_6H_2(O)\text{-}2((C(CH_3)_2((CH_2CH_3))\text{-}3,5))_2]_2$), 1.74 (1.1H, q, $[(CH_2N)(CH_2C_6H_2(O)\text{-}2((C(CH_3)_2((CH_2CH_3))\text{-}3,5))_2]_2$), 1.52 (5H, mult, $[(CH_2N)(CH_2C_6H_2(O)\text{-}2((C(CH_3)_2((CH_2CH_3))\text{-}3,5))_2]_2$), 1.44, 1.23 (6.5H, s,$[(CH_2N)(CH_2C_6H_2(O)\text{-}2((C(CH_3)_2((CH_2CH_3))\text{-}3,5))_2]_2$, 1.20 (15.9H, mult, $[(CH_2N)(CH_2C_6H_2(O)\text{-}2((C(CH_3)_2((CH_2CH_3))\text{-}3,5))_2]_2$), 1.04 (3H, s, $[(CH_2N)(CH_2C_6H_2(O)\text{-}2((C(CH_3)_2((CH_2CH_3))\text{-}3,5))_2]_2$), 0.74 (3.2H, t, $[(CH_2N)(CH_2C_6H_2(O)\text{-}2((C(CH_3)_2((CH_2CH_3))\text{-}3,5))_2]_2$, J_{H-H} = 3.6 Hz), 0.65 (6.6H, t, $[(CH_2N)(CH_2C_6H_2(O)\text{-}2((C(CH_3)_2((CH_2CH_3))\text{-}3,5))_2]_2$, J_{H-H} = 3.6 Hz), 0.39 (3.1H, t, $[(CH_2N)(CH_2C_6H_2(O)\text{-}2((C(CH_3)_2((CH_2CH_3))\text{-}3,5))_2]_2$, J_{H-H} = 3.6 Hz). Anal. Calcd for $C_{70}H_{108}N_2O_4Zr$ (MW = 1130.85): C, 74.35; H, 9.45; N, 2.47. Found: C, 73.94; H, 9.94; N, 3.45.

Hf(ED-DBP$_4$) (5). Used $Hf(OBu^t)_4$ (0.192 g, 0.536 mmol) and H_4-ED-DBP$_4$ (0.500 g, 0.536 mmol). Yield: 0.401 g (67.6%). FTIR (KBr, cm^{-1}): 2957(s), 2904(m), 2869(m), 1473(s), 1413(m), 1361(m), 1300(m), 1242(s), 1202(m), 1169(m), 1133(m), 875(m), 847(s), 809(m), 751(m), 733(m,sh), 553(m), 466(m). ^{1}H NMR (400.1 MHz, cyclo-d_{12}): δ 7.28, 7.21 (2.4H, s, $[(CH_2N)(CH_2C_6H_2(O)\text{-}2(C(CH_3)_3)_2\text{-}3,5))_2]_2$), 6.79 (2.2H, s, $[(CH_2N)(CH_2C_6H_2(O)\text{-}2(C(CH_3)_3)_2\text{-}3,5))_2]_2$, 4.37 (1.0H, d, $[(CH_2N)(CH_2C_6H_2(O)\text{-}2(C(CH_3)_3)_2\text{-}3,5))_2]_2$, J_{H-H} = 6.6 Hz), 4.14 (1.0H, d, $[(CH_2N)(CH_2C_6H_2(O)\text{-}2(C(CH_3)_3)_2\text{-}3,5))_2]_2$, J_{H-H} = 6.6 Hz), 3.07 (1.1H, d, $[(CH_2N)(CH_2C_6H_2(O)\text{-}2(C(CH_3)_3)_2\text{-}3,5))_2]_2$, J_{H-H} = 6.6 Hz), 2.95 (1.0H, d, $[(CH_2N)(CH_2C_6H_2(O)\text{-}2(C(CH_3)_3)_2\text{-}3,5))_2]_2$, J_{H-H} = 4.1 Hz), 2.80 (1.1H, d, $[(CH_2N)(CH_2C_6H_2(O)\text{-}2(C(CH_3)_3)_2\text{-}3,5))_2]_2$, J_{H-H} = 6.6 Hz), 2.47 (1.0H, d, $[(CH_2N)(CH_2C_6H_2(O)\text{-}2(C(CH_3)_3)_2\text{-}3,5))_2]_2$, J_{H-H} = 4.4 Hz), 1.52 (10.0H, s, $[(CH_2N)(CH_2C_6H_2(O)\text{-}2(C(CH_3)_3)_2\text{-}3,5))_2]_2$), 1.24, 1.22, 1.16 (33.0H, s, $[(CH_2N)(CH_2C_6H_2(O)\text{-}2(C(CH_3)_3)_2\text{-}3,5))_2]_2$). Anal. Calcd for $C_{62}H_{92}HfN_2O_4$ (MW = 1107.91): C, 67.22; H, 8.37; N, 2.53. Found: C, 66.92; H, 8.50; N, 2.31. MS(ESI+) *m/z*: $[M+H]^+$ calcd for $C_{62}H_{93}HfN_2O_4$ (MW = 1109.7): Found: 1109.7 Mp: 354 °C.

Hf(ED-DAP$_4$) (5a). Used $Hf(OBu^t)_4$ (0.225 g, 0.478 mmol) and H_4-ED-DAP$_4$ (0.500 g, 0.478 mmol). Yield: 0.195 g (33.4%). FTIR (KBr, cm^{-1}): 2963(s), 2906(m, sh), 2875(m), 1603(w), 1560(w), 1541(w), 1507(s), 1473(m, sh), 1414(m), 1384(m), 1361(m), 1267(s), 1217(w), 1199(m), 1130(w), 1037 (m, br), 873(m), 839(m), 787(m, br), 735(m), 702(m), 536(m,br), 467(m,br). ^{1}H NMR (400.1 MHz, cyclo-d_{12}, * denotes free ligand): δ 7.18, 7.14 (2.0H, s, $[(CH_2N)(CH_2C_6H_2(O)\text{-}2((C(CH_3)_2((CH_2CH_3))\text{-}3,5))_2]_2$), 6.73 (2.0H, s, $[(CH_2N)(CH_2C_6H_2(O)\text{-}2((C(CH_3)_2((CH_2CH_3))\text{-}3,5))_2]_2$), 4.31 (0.4H, d, $[(CH_2N)(CH_2C_6H_2(O)\text{-}2((C(CH_3)_2((CH_2CH_3))\text{-}3,5))_2]_2$, J_{H-H} = 6.6 Hz), 4.14 (0.4H, d, $[(CH_2N)(CH_2C_6H_2(O)\text{-}2((C(CH_3)_2((CH_2CH_3))\text{-}3,5))_2]_2$, J_{H-H} = 6.5 Hz), 4.01* (0.4H, s, $[(CH_2N)(CH_2C_6H_2(OH)\text{-}2((C(CH_3)_2((CH_2CH_3))\text{-}3,5))_2]_2$), 3.43* (0.7H, s, $[(CH_2N)(CH_2C_6H_2(OH)\text{-}2((C(CH_3)_2((CH_2CH_3))\text{-}3,5))_2]_2$), 3.03 (0.9H, d, $[(CH_2N)(CH_2C_6H_2(O)\text{-}2((C(CH_3)_2((CH_2CH_3))\text{-}3,5))_2]_2$, J_{H-H} = 6.7 Hz), 2.86 (0.7H, d, $[(CH_2N)(CH_2C_6H_2(O)\text{-}2((C(CH_3)_2((CH_2CH_3))\text{-}3,5))_2]_2$, J_{H-H} = 4.4 Hz), 2.75 (0.4H, d, $[(CH_2N)(CH_2C_6H_2(O)\text{-}2((C(CH_3)_2((CH_2CH_3))\text{-}3,5))_2]_2$, J_{H-H} = 6.6 Hz), 2.64 (0.3H, d, $[(CH_2N)(CH_2C_6H_2(O)\text{-}2((C(CH_3)_2((CH_2CH_3))\text{-}3,5))_2]_2$, J_{H-H} = 4.4 Hz), 2.29 (1.0H, mult., $[(CH_2N)(CH_2C_6H_2(O)\text{-}2((C(CH_3)_2((CH_2CH_3))\text{-}3,5))_2]_2$), 2.02 (1.0H, mult., $[(CH_2N)(CH_2C_6H_2(O)\text{-}2((C(CH_3)_2((CH_2CH_3))\text{-}3,5))_2]_2$), 1.55, 1.45, 1.44, 1.32 (16.3H, s, $[(CH_2N)(CH_2C_6H_2(O)\text{-}2((C(CH_3)_2((CH_2CH_3))\text{-}3,5))_2]_2$), 1.19 (17.3H, t, $[(CH_2N)(CH_2C_6H_2(O)\text{-}2((C(CH_3)_2((CH_2CH_3))\text{-}3,5))_2]_2$, J_{H-H} = 3.5 Hz), 0.74 (1.8H, t. $[(CH_2N)(CH_2C_6H_2(O)\text{-}2((C(CH_3)_2((CH_2CH_3))\text{-}3,5))_2]_2$, J_{H-H} = 3.7 Hz), 0.63 (18.2H, t, $[(CH_2N)(CH_2C_6H_2(O)\text{-}2((C(CH_3)_2((CH_2CH_3))\text{-}3,5))_2]_2$, J_{H-H} = 3.6 Hz), 0.39 (1.8H, t, $[(CH_2N)(CH_2C_6H_2(O)\text{-}2((C(CH_3)_2((CH_2CH_3))\text{-}3,5))_2]_2$, J_{H-H} = 3.7 Hz). Anal. Calcd for $C_{70}H_{108}HfN_2O_4$ (MW = 1218.76): C, 68.91; H, 8.92; N, 2.30. Found: C, 68.56; H, 9.35; N, 3.35.

Ti(ED-DCP$_4$) (6). Used $Ti(OPr^i)_4$ (0.186 g, 0.658 mmol) and H_4-ED-DCP$_4$ (0.500 g, 0.658 mmol). Crystalline Yield: 0.358 g (67.6%). FTIR (KBr, cm^{-1}): 2961(w), 2920(w), 2872(w), 1625(w), 1585(w), 1560(w), 1422(s), 1317(m,sh), 1296(m,sh), 1270(m), 1217(m), 1181(m), 1096(w), 1029(w), 962(w), 871-(s),776(s), 579(m), 561(m), 505(m). ^{1}H NMR (400.1 MHz, py-d_5): δ 7.24, 7.23 (1.1H, s, $[(CH_2N)(CH_2C_6H_2(O)\text{-}2(Cl)_2\text{-}3,5))_2]_2$), 6.94, 6.93 (1.0H, s, $[(CH_2N)(CH_2C_6H_2(O)\text{-}2(Cl)_2\text{-}3,5))_2]_2$), 4.73 (1.0H, d, $[(CH_2N)(CH_2C_6H_2(O)\text{-}2(Cl)_2\text{-}3,5))_2]_2$, J_{H-H} = 7.1 Hz), 3.92 (1.1H, d, $[(CH_2N)(CH_2C_6H_2(O)\text{-}2(Cl)_2\text{-}3,5))_2]_2$, J_{H-H} = 7.0 Hz), 3.81 (1.0H, d, $[(CH_2N)(CH_2C_6H_2(O)\text{-}2(Cl)_2\text{-}3,5))_2]_2$, J_{H-H} = 7.2 Hz), 3.65 (1.0H, d, $[(CH_2N)(CH_2C_6H_2(O)\text{-}2(Cl)_2\text{-}3,5))_2]_2$, J_{H-H} = 7.1 Hz), 3.10 (1.0H, d, $[(CH_2N)(CH_2C_6H_2(O)\text{-}2(Cl)_2\text{-}3,5))_2]_2$, J_{H-H} = 5.0 Hz), 3.01 (1.0H, d, $[(CH_2N)(CH_2C_6H_2(O)\text{-}2(Cl)_2\text{-}3,5))_2]_2$, J_{H-H} = 5.0 Hz). Anal. Calcd for $C_{30}H_{20}Cl_8N_2O_4Ti$ (MW = 803.98): C, 44.81; H, 2.51; N, 3.48. Found: C, 46.81; H, 2.89; N, 2.79. MS(ESI+) *m/z*: $[M+H]^+$ calcd for $C_{30}H_{21}Cl_8N_2O_4Ti$ (MW = 800.8). Found: 800.9. Mp: > 360 °C.

Zr(ED-DCP$_4$)(py)$_2$ (7). Used Zr(OBu^t)$_4$ (0.252 g, 0.658 mmol) and H$_4$-ED-DCP$_4$ (0.500 g, 0.658 mmol). Crystalline Yield: 0.103 g (15.6%). FTIR (KBr, cm^{-1}): 3077(m), 2960(m), 2890(m), 2854(m), 1606(w), 1585(m), 1559(m), 1461(s), 1384(m), 1366(m), 1309(s), 1284(s), 1255(m), 1219(m), 1181(m), 1098(m), 1070(m), 1042(m), 1014(m), 865(s), 770(s), 732(m,sh), 695(m), 571(m), 467(m). ^{1}H NMR (400.1 MHz, cyclo-d_{12}): δ 9.21 (1.2H, d, C_5H_5N), 7.63 (0.6H, t, C_5H_5N), 7.25(1.2H, C_5H_5N), 7.10 (0.8H, s, [(CH$_2$N)(CH$_2$C$_6$*H*$_2$(O)-2(Cl)$_2$-3,5))$_2$]$_2$), 6.92 (0.8H, s, [(CH$_2$N)-(CH$_2$C$_6$*H*$_2$(O)-2(Cl)$_2$-3,5))$_2$]$_2$), 6.67(1.0H, s, [(CH$_2$N)(CH$_2$C$_6$*H*$_2$-(O)-2(Cl)$_2$-3,5))$_2$]$_2$), 6.56(1.0H, s, [(CH$_2$N)(CH$_2$C$_6$*H*$_2$(O)-2(Cl)$_2$-3,5))$_2$]$_2$), 4.57 (1.0H, d, [(CH$_2$N)(C*H*$_2$C$_6$H$_2$(O)-2(Cl)$_2$-3,5))$_2$]$_2$, J_{H-H} = 6.6 Hz), 3.75 (1.0H, d, [(CH$_2$N)(C*H*$_2$C$_6$H$_2$(O)-2(Cl)$_2$-3,5))$_2$]$_2$, J_{H-H} = 6.6 Hz), 3.07 (1.0H, d, [(CH$_2$N)(C*H*$_2$C$_6$H$_2$(O)-2(Cl)$_2$-3,5))$_2$]$_2$, J_{H-H} = 6.6 Hz), 2.91 (1.0H, d, [(CH$_2$N)-(C*H*$_2$C$_6$H$_2$(O)-2(Cl)$_2$-3,5))$_2$]$_2$, J_{H-H} = 6.6 Hz), 2.65 (1.0H, br s, [(C*H*$_2$N)(CH$_2$C$_6$H$_2$(O)-2(Cl)$_2$-3,5))$_2$]$_2$), 2.50(1.0H, br s, [(C*H*$_2$N)-(CH$_2$C$_6$H$_2$(O)-2(Cl)$_2$-3,5))$_2$]$_2$). Anal. Calcd for $C_{40}H_{30}Cl_8N_4O_4Zr$ (MW = 1005.50): C, 47.78; H, 3.01; N, 5.57. Found: C, 47.33; H, 2.72; N, 4.40. MS(ESI+) *m*/*z*: [M+H]$^+$ calcd for $C_{30}H_{20}Cl_8N_2O_4Zr$ (MW = 842.8). Found: 842.8. Mp: 250 °C.

(HOBu^t)Hf(ED-DCP$_4$) (8). Used Hf(OBu^t)$_4$ (0.236 g, 0.658 mmol) and H$_4$-ED-DCP$_4$ (0.500 g, 0.658 mmol). Yield: 0.429 g (64.7%). FTIR (KBr, cm^{-1}): 3488 (s), 2965(m), 2923(m), 2905(m), 2868(m), 1621(w), 1589(m), 1562(w), 1468(s), 1381(m), 1370(m), 1317(m), 1286(m), 1256(m), 1219(m), 1028(m), 866(s), 771(m), 572(m), 462(m). ^{1}H NMR (400.1 MHz, cyclo-d_{12}): δ 7.34 (1.9H, mult., [(CH$_2$N)(CH$_2$C$_6$*H*$_2$(O)-2(Cl)$_2$-3,5))$_2$]$_2$), 6.74 (1.0H, s, [(CH$_2$N)(CH$_2$C$_6$*H*$_2$(O)-2(Cl)$_2$-3,5))$_2$]$_2$), 6.60 (0.9H, s, [(C*H*$_2$N)(CH$_2$C$_6$H$_2$(O)-2(Cl)$_2$-3,5))$_2$]$_2$), 4.63 (0.8H, d, [(CH$_2$N)(C*H*$_2$C$_6$H$_2$(O)-2(Cl)$_2$-3,5))$_2$]$_2$, J_{H-H} = 6.6 Hz), 3.92 (0.7H, d, [(CH$_2$N)(C*H*$_2$C$_6$H$_2$(O)-2(Cl)$_2$-3,5))$_2$]$_2$, J_{H-H} = 6.3 Hz), 3.08 (0.8H, d, [(CH$_2$N)(C*H*$_2$C$_6$H$_2$(O)-2(Cl)$_2$-3,5))$_2$]$_2$, J_{H-H} = 6.4 Hz), 2.99 (1.10H, d, [(CH$_2$N)(C*H*$_2$C$_6$H$_2$(O)-2(Cl)$_2$-3,5))$_2$]$_2$, J_{H-H} = 6.6 Hz), 2.66, 2.58 (1.5H, br s, [(C*H*$_2$N)-(CH$_2$C$_6$H$_2$(O)-2(Cl)$_2$-3,5))$_2$]$_2$), 1.38 (s, HOC(C*H*$_3$)$_3$, shoulder on cyclo-d_{12} resonance). Anal. Calcd for $C_{34}H_{30}Cl_8HfN_2O_5$ (MW = 1008.69): C, 40.48; H, 3.00; N, 2.78. Found: C, 40.02; H, 4.65; N, 1.92. Mp: 250 °C.

General Synthesis. Because of the similarity of synthesis of **9a**−**13**, a general description is supplied for this set of compounds. The desired H$_4$-ED-L$_4$ was slowly added to a stirring solution of the metal precursor dissolved in tol (∼5 mL). The reactions were allowed to stir for 12 h. If a precipitate was present, THF or py was added to the reaction until clear. If the precipitate persisted, then the reaction was gently warmed until the reaction was clear. After cooling to room temperature, if crystals did not grow, the volatile portion of the reaction was allowed to slowly evaporate until crystals formed.

[(THF)Ca]$_2$[ED-(DBP)$_2$(μ_c-DBP)$_2$] (9a) and {[(py)Ca[ED-(μ-DBP-η^5)$_4$Ca]$_2$}$_n$ (9b). Used Ca(NR$_2$)$_2$ (0.400 g, 1.11 mmol) and H$_4$-ED-DBP$_4$ (0.519 g, 0.160 mmol). Crystals isolated from THF were **9a**. FTIR (KBr, cm^{-1}): 2861(s), 2781(m), 1703(m), 1654(m), 1471(s), 1439(s), 1383(m), 1362(m), 1319(m), 1158(s), 1079(m), 1025(m), 856(m), 825(m), 805(m), 571(m), 471(m). Crystals isolated from py were found to be **9b**. Yield: 0.456 g (81.4%). FTIR (KBr, cm^{-1}): 2957(s), 2902(s), 2868(s), 2794(s), 1592(m), 1473(s), 1439(s), 1361(m), 1317(s), 1295(s), 1258(w), 1233(w), 1201(w), 1150(m), 1105(w), 1031(w), 998(w), 934 (w), 882(m), 829(w), 750(m), 703(w), 650(w), 572(m), 548(m), 505(w), 405(m). ^{1}H NMR (400.1 MHz, py-d_5): δ 8.70, 7.54, 7.18 (NC$_5$-*H*$_5$), 7.39 (1.0H, s, [(CH$_2$N)(CH$_2$C$_6$*H*$_2$(O)-2(C(CH$_3$)$_3$)$_2$-3,5))$_2$]$_2$), 3.84−3.50 (mult (br), [(CH$_2$N)(C*H*$_2$C$_6$H$_2$(O)-2(C(CH$_3$)$_3$)$_2$-3,5))$_2$]$_2$), 2.93 (1.0H, s, [(C*H*$_2$N)(CH$_2$C$_6$H$_2$(O)-2(C(CH$_3$)$_3$)$_2$-3,5))$_2$]$_2$), 1.59 (10H, s, [(C*H*$_2$N)(CH$_2$C$_6$H$_2$(O)-2(C(CH$_3$)$_3$)$_2$-3,5))$_2$]$_2$), 1.59 (13H, s, [(CH$_2$N)(CH$_2$C$_6$H$_2$(O)-2(C(C*H*$_3$)$_3$)$_2$-3,5))$_2$]$_2$), 1.41 (13H, s, [(CH$_2$N)(CH$_2$C$_6$H$_2$(O)-2(C(C*H*$_3$)$_3$)$_2$-3,5))$_2$]$_2$). Anal. Calcd for $C_{62}H_{92}Ca_2N_2O_4$ (MW = 1009.58): C, 73.76; H, 9.19; N, 2.77. Found: C, 79.55; H, 8.64; N, 5.39.

[(py)Zn][ED-(DBP)$_4$][Zn(py)$_2$] (10)·•5py. Used Zn(Et)$_2$ (0.856 mL, 0.856 mmol) and H$_4$-ED-DBP$_4$ (0.400 g, 0.428 mmol). Yield: 0.402 g (55.5%). FTIR (KBr, cm^{-1}): 2955(s), 2913(m), 2866(m), 1604(w), 1474(m), 1441(m), 1362(w), 1302(w), 1240(m), 1205(m), 1102(w), 1070(w), 875(w), 834(w), 805(w), 742(m), 704(m), 476(m), 431(s). ^{1}H NMR (400.1 MHz, py-d_5): δ 8.70, 7.54, 7.18 (NC$_5$*H*$_5$), 7.49 (1.0H, s, [(CH$_2$N)(CH$_2$-C$_6$*H*$_2$(O)-2(C(CH$_3$)$_3$)$_2$-3,5))$_2$]$_2$), 6.82 (0.9H, s, [(CH$_2$N)(CH$_2$-C$_6$*H*$_2$(O)-2(C(CH$_3$)$_3$)$_2$-3,5))$_2$]$_2$), 4.20−2.80 (mult (br), [(CH$_2$N)-(C*H*$_2$C$_6$H$_2$(O)-2(C(CH$_3$)$_3$)$_2$-3,5))$_2$]$_2$), 3.02 (1.0H, s, [(C*H*$_2$N)-(CH$_2$C$_6$H$_2$(O)-2(C(CH$_3$)$_3$)$_2$-3,5))$_2$]$_2$), 1.59 (10H, s, [(C*H*$_2$N)-(CH$_2$C$_6$H$_2$(O)-2(C(CH$_3$)$_3$)$_2$-3,5))$_2$]$_2$), 1.34 (11H, s, [(CH$_2$N)-(CH$_2$C$_6$H$_2$(O)-2(C(C*H*$_3$)$_3$)$_2$-3,5))$_2$]$_2$), 1.19 (9H, s, [(CH$_2$N)(CH$_2$-C$_6$H$_2$(O)-2(C(C*H*$_3$)$_3$)$_2$-3,5))$_2$]$_2$). Anal. Calcd for $C_{102}H_{132}N_{10}O_4Zn_2$ (MW = 1692.92): C, 72.36; H, 7.85; N, 8.27. Found: C, 69.12; H, 8.19; N, 5.58.

[(py)Sn]$_2$[ED-(DBP)$_4$] (11). Used Sn(NMe$_2$)$_2$ (0.544 g, 4.83 mmol): and H$_4$-ED-DBP$_4$ (2.25 g, 2.42 mmol). Yield: 0.998 g (31.1%). FTIR (KBr, cm^{-1}): 2955(s), 2915(s), 2862(s), 2752(w), 2709(w), 2664(w), 1602(m,br), 1541(m), 1521(m), 1472(s), 1442(s), 1411(m), 1360(m), 1294(m,sh), 1244(s), 1208(m), 1126(m), 1099(m), 1025(m), 983(w), 958(w), 878(w), 841(m), 795(m), 746(m), 729(m), 663(m), 612(m), 585(w), 555(m), 532(w), 513(w), 542(m). ^{1}H NMR (400.1 MHz, py-d_5): δ 8.71, 7.54, 7.18 (NC$_5$*H*$_5$), 7.06 (1.4H, s, [(CH$_2$N)(CH$_2$C$_6$*H*$_2$(O)-2(C-(CH$_3$)$_3$)$_2$-3,5))$_2$]$_2$), 4.97 (1.0H, d, [(CH$_2$N)(C*H*$_2$C$_6$H$_2$(O)-2(C-(CH$_3$)$_3$)$_2$-3,5))$_2$]$_2$, J_{H-H} = 6.2 Hz), 3.79 (1.0H, d, [(CH$_2$N)-(C*H*$_2$C$_6$H$_2$(O)-2(C(CH$_3$)$_3$)$_2$-3,5))$_2$]$_2$, J_{H-H} = 6.2 Hz), 3.56 (0.9H, s, [(C*H*$_2$N)(CH$_2$C$_6$H$_2$(O)-2(C(CH$_3$)$_3$)$_2$-3,5))$_2$]$_2$), 1.61 (15.5H, s, [(CH$_2$N)(CH$_2$C$_6$H$_2$(O)-2(C(C*H*$_3$)$_3$)$_2$-3,5))$_2$]$_2$), 1.45 (16.9H, s, [(CH$_2$N)(CH$_2$C$_6$H$_2$(O)-2(C(C*H*$_3$)$_3$)$_2$-3,5))$_2$]$_2$). Anal. Calcd for $C_{72}H_{102}N_4O_4Sn_2$ (MW = 1324.96): C, 65.26; H, 7.76; N, 4.23. Found: C, 62.52; H, 7.28; N, 5.66.

[(py)(ONep)$_2$Ti(ED-DBP$_4$)Zn(py)] (12). Used sequential addition of Zn(Et)$_2$ (0.500 mL, 0.500 mmol) followed by [Ti(ONep)$_4$)]$_2$ (0.198 g, 0.500 mmol) to H$_4$-ED-DBP$_4$ (0.467 g, 0.500 mmol). Yield: 0.368 g (53.5%). FTIR (KBr, cm^{-1}): 2956(s), 2905(m), 2884(m), 1605(w), 1473(m), 1444(m), 1362(w), 1262(m), 1203(m), 1167(w), 1099(m), 1042(m), 851(w), 832(w), 755(w), 682(w), 456(s), 431(s). Anal. Calcd for $C_{82}H_{124}N_4O_6TiZn$ (MW = 1375.12): C, 71.62; H, 9.09; N, 4.07. Found: C, 67.41; H, 8.61; N, 4.13.

(py)Li[ED-(DBP)$_3$(H-DBP)]Co (13). Used Co[μ-OC$_6$H$_4$(CH-Me$_2$)$_2$-2)$_2$Li(py)$_2$]$_2$ (0.350 g, 0.376 mmol) and H$_4$-ED-DBP$_4$ (0.351 g, 0.376 mmol). Yield: 0.226 g (55.9%). FTIR (KBr, cm^{-1}): 2966(s), 2924(s), 2863(s), 1594(s), 1483(s), 1493(s), 1385(w), 1356(w), 1290-(s), 1254(s), 1149(w), 1095(m), 1024(s), 899(m), 896(m), 836(s), 798(m), 748(s), 706(s), 667(m), 641(m), 893(s), 555(m), 501(s), 481(s). Anal. Calcd for $C_{67}H_{98}CoLiN_3O_4$ (MW = 1075.35): C, 74.83; H, 9.19; N, 3.91. Found: C, 71.73; H, 9.71; N, 2.74.

General X-ray Crystal Structure Information.[39] Crystals were mounted onto a glass fiber from a pool of Fluorolube and immediately placed in a cold N$_2$ vapor stream, on a Bruker AXS diffractometer equipped with a SMART 1000 CCD detector using graphite monochromatized Mo Kα radiation (λ = 0.7107 Å). Lattice determination and data collection were carried out using SMART Version 5.054 software. Data reduction was performed using SAINTPLUS Version 6.01 software and corrected for absorption using the SADABS program within the SAINT software package.

Structures were solved by direct methods that yielded the heavy atoms, along with a number of the lighter atoms or by using the PATTERSON method, which yielded the heavy atoms. Subsequent Fourier syntheses yielded the remaining light-atom positions. The hydrogen atoms were fixed in positions of ideal geometry and refined using SHELXL software.

(39) Boyle, T. J.; Alam, T. M.; Tafoya, C. J.; Mechenbier, E. R.; Ziller, J. W. *Inorg. Chem.* **1999**, *38*, 2422.

The final refinement of each compound included anisotropic thermal parameters for all non-hydrogen atoms. It is of note that crystal structures of $M(OR)_x$ often contain disorder within the atoms of the ligand chain causing higher than normal final correlations.[2,4−8,21−26,28−31,40,41] All CIF files were checked at http://www.iucr.org/. Additional information concerning the data collection and final structural solutions can be found in the Supporting Information or by accessing CIF files through the Cambridge Crystallographic Data Base. Data collection parameters for **1**−**8** and **9a**−**13** are given in Tables 1 and 2, respectively. For the final structural solution for compound **2** disordered solvent and *t*-butyl groups were noted that resulted in slightly larger refinement parameters. Compounds **4**, **4a**, **6**, **7**, **8**, **9a**, **11**, **12**, and **13** were found to possess a void error based on an enlarged area that does *not* contain a solvent molecule. For **6** and **9b** disordered solvent molecules were necessarily removed by Squeeze/Platon to solve the structure.

Results and Discussion

A survey of structurally characterized metal ED-L_4 derivatives revealed that only a handful of these compounds have been disseminated, including [Zn(ED-DMP_3(H-DMP))]-[Na][35] and [Fe(ED-Bz_4)][$NHEt_3$],[36] V(ED-Bz_4)•(CH_2Cl_2)[37] and Ti(ED-Bz_4)•(CH_2Cl_2)[38] where H_4-ED-DMP_4 = [tetra(3,5-dimethylbenzyl-2-hydroxybenzyl)-*N*,*N*′-ethylenediamine] and H_4-ED-Bz_4 = [tetra(2-hydroxy benzyl)-*N*,*N*′-ethylenediamine]. Because of the paucity of structures available and the recently reported simple, synthetic route to substituted H_4-ED-L_4 species,[35] a study of the coordination chemistry of ED-L_4 species with the group 4 cations was undertaken. This family of cations was selected based on their ubiquity in ceramic applications and the fact that the unsubstituted species show complete encapsulation of the metal for Ti(ED-Bz_4)•(CH_2Cl_2).[38] This behavior is intriguing since it could be used as a means to control the chemistry of $M(OR)_x$, if tuned properly.

One possible method that can be used to alter the coordination behavior is to vary the cation size without changing the charge. In addition to the cation fine-tuning approach, significant structural variations of metal aryloxide derivatives have been observed based on *ortho* substitutions in the ring.[12,42−46] Using these approaches, the coordination chemistries of the $M(OR)_4$ derivatized by the H_4-ED-L_4 ligands have been determined for the first time. The synthesis and characterization of the resultant products of eq 1 are discussed below.

Synthesis. Ligands. The H_4-ED-L_4 derivatives were synthesized using a one-pot Mannich Condensation reaction. The reaction employed 6 equiv of the appropriate substituted phenol, ethylene diamine, and 4 equiv of paraformaldehyde that was heated, without solvent at 80 °C for 3 days.[35] From a concentrated solution of py, crystals of **1** •2py (Figure 2) and **2** •2py (Figure 3), were isolated, confirming their connectivity. This family of multidentate ligands (**1**, **1a**, and **2**) possessing 6 heteroatoms (4 oxygens and 2 nitrogens) are quite flexible and capable of binding transition metals with charges that could, depending on the degree of de/protonation, vary from −4 to +2. The binding of the amine and phenolate groups of the ED-L_4 ligands to a metal center can result in the formation of a series of thermodynamically favored five-member rings. In addition, the flexible backbone should allow these ligands to accommodate a wide variety of cation sizes (vide infra). Therefore, the exploration of the coordination of **1**, **1a**, and **2** with $M(OR)_4$ was undertaken.

Metal Complexes. The structural changes wrought by the steric variations of the alkyl substituents on the phenoxide rings of the ED-L_4 (L = DBP (**1**) or DAP (**1a**)) upon reacting with $Ti(OR)_4$ were investigated. Initially, compound **1** was independently mixed in tol (eq 1) with a series of sterically varied $Ti(OR)_4$ (OR = OPr^i, *neo*-pentoxide (ONep), and OBu^t). Irrespective of the starting material or the stoichiometry of the initial reaction, the crystals isolated possessed the same FTIR spectrum. The bends and stretches noted for these compounds were similar to **1** minus the OH stretches, coupled with the appearance of Ti−O stretches.[18,19,27,28] Single crystal X-ray crystal studies revealed that the product was **3**. The Ti metal center of compound **3** is completely encapsulated by a single ED-DBP_4 yielding an octahedral (O_h) environment: axially by two O from two phenoxide moieties and equatorially by two O from the other phenoxides along with two N of the ethylene diamine backbone. The metrical data of **3** and the Ti(ED-Bz_4)•(CH_2Cl_2)[38] derivative are in agreement with each other (see Table 3). It is of note that there are two independent molecules of **3** in the final unit cell solution.

$$\underset{(1,\,1a,\,2)}{M(OR)_4} + \underset{}{H_4\text{-ED-}L_4} \rightarrow \underset{(3-8)}{M(\text{ED-}L_4)} \qquad (1)$$

Since the O_h bound Zr^{4+} (0.86 Å) and Hf^{4+} (0.85 Å) cations are substantially larger in size than that of Ti^{4+} (0.75 Å),[47] it was of interest to see how altering the metal would affect the coordination behavior of **1**. The group 4 congeners, $Zr(OBu^t)_4$ and $Hf(OBu^t)_4$ were reacted in a similar manner (eq 1). The FTIR data and the single crystal X-ray structures indicated that both the Zr species **4** and the Hf derivative **5** (see Figure 4) were structurally similar to **3**.

Switching from the Bu^t derivative **1** to the amyl derivative **1a** in eq 1, yielded **4a** for Zr, (Figure 5) and **5a** for Hf. The species isolated were similar in structure to **3**−**5** with no impact on the general structure type imparted from the change to an amyl group. The **1a** derivative of Ti formed an oil that could not be crystallized in our hands. While the structural data of **5a** was not of high enough quality to allow for a finalized structure to be reported, the connectivity was unequivocally established as a mononuclear species, and the unit cell information for

(40) Bradley, D. C.; Mehrotra, R. C.; Rothwell, I. P.; Singh, A. *Alkoxo and Aryloxo Derivatives of Metals*; Academic Press: New York, 2001; p 704.
(41) Turova, N. Y.; Turevskaya, E. P.; Kessler, V. G.; Yanovskaya, M. I. *The Chemistry of Metal Alkoxide*; Kluwer Academic Publishers: Boston, 2002; p 568.
(42) Boyle, T. J.; Andrews, N. L.; Rodriguez, M. A.; Campana, C.; Yiu, T. *Inorg. Chem.* **2003**, *42*, 5357.
(43) Boyle, T. J.; Pedrotty, D. M.; Alam, T. M.; Vick, S. C.; Rodriguez, M. A. *Inorg. Chem.* **2000**, *39*, 5133.
(44) Boyle, T. J.; Andrews, N. L.; Alam, T. M.; Rodriguez, M. A.; Santana, J. M.; Scott, B. L. *Polyhedron* **2002**, *21*, 2333.
(45) Boyle, T. J.; Hernandez-Sanchez, B. A.; Baros, C. M.; Brewer, L. N.; Rodriguez, M. A. *Chem. Mater.* **2007**, *19*, 2016.
(46) Boyle, T. J.; Bunge, S. D.; Clem, P. G.; Richardson, J.; Dawley, J. T.; Ottley, L. A. M.; Rodriguez, M. A.; Tuttle, B. A.; Avilucea, G. R.; Tissot, R. G. *Inorg. Chem.* **2005**, 44.
(47) Shannon, R. D. *Acta Crystallogr.* **1976**, *A32*, 751.

Table 1. Data Collection Parameters for **1**−**8**

	1 •2py	**2** •2py	**3**	**4**	**4a**
chemical formula	$C_{72}H_{106}N_4O_4$	$C_{40}H_{34}Cl_8N_4O_4$	$C_{62}H_{92}N_2O_4Ti$	$C_{62}H_{92}N_2O_4Zr$	$C_{70}H_{106}N_2O_4Zr$
formula weight	1091.63	918.31	977.28	1020.60	1130.85
temp (K)	173(2)	173(2)	170(2)	173(2)	173(2)
space group	monoclinic, *P*2(1)/*c*	triclinic, $P\bar{1}$	monoclinic, *C*2/*c*	triclinic, $P\bar{1}$	triclinic, $P\bar{1}$
a (Å)	14.705(3)	10.7518(16)	63.71(2)	12.7714(18)	13.2250(18)
b (Å)	27.786(5)	10.8145(16)	14.575(5)	14.633(2)	15.259(2)
c (Å)	9.5561(17)	19.060(3)	23.940(8)	21.570(3)	18.747(3)
α (deg)		100.602(2)		98.404(2)	81.881(2)
β (deg)	102.421(4)	98.922(2)	93.117(10)	101.158(2)	78.100(2)
γ (deg)		100.306(2)		110.041(2)	75.794(2)
V (Å^3)	3813.0(12)	2102.3(5)	22198(12)	3615.3(9)	3572.3(8)
Z	2	2	12	2	2
D_{calcd}(Mg/m^3)	1.089	1.451	0.877	0.938	1.051
μ,(Mo, Kα) (mm^{-1})	0.066	0.582	0.151	0.189	0.197
R1[a] (%) (all data)	12.96 (18.62)	6.78 (7.33)	10.83 (13.13)	4.66 (5.51)	8.07 (9.50)
wR2[b] (%) (all data)	36.02 (39.20)	18.73 (19.49)	26.71 (28.15)	12.28 (12.69)	20.93 (21.90)

	5	**5a**	**6**	**7**	**8**
chemical formula	$C_{62}H_{92}HfN_2O_4$	$C_{70}H_{106}HfN_2O_4$	$C_{30}H_{20}Cl_8N_2O_4Ti$	$C_{40}H_{30}Cl_8N_4O_4Zr$	$C_{34}H_{30}Cl_8HfN_2O_5$
formula weight	1106.86	1218.76	803.98	1005.50	1008.69
temp (K)	173(2)	173(2)	166(2)	173(2)	173(2)
space group	triclinic, $P\bar{1}$	triclinic, $P\bar{1}$	triclinic, $P\bar{1}$	monoclinic, *C*2/*c*	triclinic, $P\bar{1}$
a (Å)	12.7118(8)	13.1949	8.7072(18)	37.711(7)	9.3452(11)
b (Å)	14.6046(9)	15.2330	9.1709(19)	16.607(3)	9.5899(11)
c (Å)	21.5762(13)	18.7763	22.757(5)	20.967(4)	22.693(3)
α (deg)	98.2460(10)	82.2138	80.087(4)		88.851(2)
β (deg)	101.3170(10)	78.1811	85.933(4)	90.565(3)	86.734(2)
γ (deg)	109.9060(10)	76.1184	77.230(4)		82.537(2)
V (Å^3)	3595.8(4)	3571.25	1744.8(6)	13130(4)	2013.1(4)
Z	2	dno[c]	2	8	2
D_{calcd}(Mg/m^3)	1.022	dno[c]	1.530	1.017	1.664
μ,(Mo, Kα) (mm^{-1})	1.487	dno[c]	0.895	0.523	3.163
R1[a] (%) (all data)	3.03 (3.33)	dno[c]	6.01 (8.57)	4.18(6.39)	5.10 (5.53)
wR2[b] (%) (all data)	7.81 (7.94)		13.58 (14.72)	10.24(10.87)	12.66 (12.92)

[a] $R1 = \sum||F_o| - |F_c||/\sum|F_o| \times 100$. [b] $wR2 = [\sum w(F_o^2 - F_c^2)^2/\sum w(F_o^2)^2]^{1/2} \times 100$. [c] dno = data not obtained.

Table 2. Data Collection Parameters for **9**−**13**

	9a	**9b**	**10** •5py	**11**	**12**	**13**
chemical formula	$C_{70}H_{108}Ca_2N_2O_6$	$C_{62}H_{92}Ca_2N_2O_4$	$C_{102}H_{132}N_{10}O_4Zn_2$	$C_{72}H_{102}N_4O_4Sn_2$	$C_{82}H_{124}N_4O_6TiZn$	$C_{67}H_{98}CoLiN_3O_4$
formula weight	1153.74	1009.58	1692.92	1324.96	1375.12	1075.35
temp (K)	173(2)	173(2)	173(2)	173(2)	173(2)	173(2)
space group	monoclinic, *P*2(1)/*n*	triclinic, *P*1	monoclinic, *Pn*	monoclinic, *P*2(1)/*c*	orthorhombic, *P*2(1)2(1)2(1)	monoclinic, *P*2(1)/*n*
a (Å)	13.977(3)	14.4298	17.903(4)	13.528(4)	15.7735(19)	13.5926(17)
b (Å)	25.017(4)	14.4425	16.852(4)	11.331(3)	18.608(2)	36.508(5)
c (Å)	24.951(4)	20.1667	17.986(4)	27.606(8)	39.651(5)	14.9240(19)
		97.093				
β (deg)	92.286(4)	97.106	118.968(3)	99.106(5)		91.523(3)
		113.549				
V (Å^3)	8718(3)	dno[c]	4747.6(17)	4178(2)	11638(2)	7403.3(16)
Z	4	dno[c]	2	2	4	4
D_{calcd}(Mg/m^3)	0.879	dno[c]	1.184	1.053	0.785	0.965
μ,(Mo, Kα) (mm^{-1})	0.169	dno[c]	0.560	0.638	0.310	0.272
R1[a] (%) (all data)	7.27 (15.84)	dno[c]	4.89 (5.53)	7.09(7.67)	6.18 (8.54)	5.25 (7.87)
wR2[b] (%) (all data)	16.84 (19.55)		11.39 (11.81)	19.04(19.31)	13.15 (14.19)	14.41 (15.22)

[a] $R1 = \sum||F_o| - |F_c||/\sum|F_o| \times 100$. [b] $wR2 = [\sum w(F_o^2 - F_c^2)^2/\sum w(F_o^2)^2]^{1/2} \times 100$. [c] dno = data not obtained.

5a is supplied (Table 1) to assist in its identification. The metrical data (Table 3) of **3**−**5** are self-consistent and within the expected distances and angle ranges for the literature compounds,[37,38] when the cation size variations are taken into account.[47]

Because of the lack of variation noted for **3**−**5a**, it was of interest to determine the effect that the electron withdrawing chlorine modified ED-L_4 of **2** would impart to the final structure. Upon addition of **2** to the M(OBu^t)$_4$ (M = Ti, Zr, Hf) precursors highly colored solutions for both Ti and Zr and a pale colored solution for Hf were obtained. The FTIR spectra for the crystals isolated indicated that no −OH peaks were present for **6** or **7** but a substantial −OH peak was noted in the spectrum of **8** at 3488 cm^{-1}. The crystal structure of the smallest cation Ti (**6**), proved to be similar to the ED-DBP_4 derivative with complete encapsulation of the metal by the hexadentate ligand ED-DCP_4 (Figure 6). In contrast,

the Zr cation yielded **7** (Figure 7) with the expected hexacoordinated ED-DCP_4 and surprisingly 2 py solvent molecules resulting in a disordered 8-coordinated metal center. The ability to add solvent molecules in the presence of the ED-L_4 ligand is attributed to the larger cation size of Zr (0.86 Å) in comparison to Ti (0.745 Å).[47] The open coordination site was verified with the isolation of **8**, wherein in addition to the ED-DCP_4 ligand, a molecule of H-OBu^t was found bound to the Hf (Figure 8). The $HOBu^t$ must have been generated in situ from the alcoholysis of the starting $Hf(OBu^t)_4$ starting material. It is believed the steric bulk of the H-OBu^t prevents the binding of additional solvent molecules as noted for **7**, since 6-coordinated Zr and Hf possess similar cation sizes.[47]

For **3**−**8**, because of the nature of the ED-L_4 ligand, there is the potential for the introduction of a "handedness" upon complexation leading to Δ and Λ configurations as noted for EDTA derivatives.[48] However, structures **3**−**8** were solved in centrosymmetric space groups and thus contain equal numbers of Δ and Λ molecules (i.e., racemic). Compounds **10** and **12** were isolated in non-centrosymmetric space groups with a Flack parameter of 10 and 0.054(13), respectively. The large parameter noted for **10** is well outside the expected range of 0.0−1.0, which renders the absolute structure parameter meaningless because of the compounds' weak anomalous scattering. However, for **12**, the value indicates that the absolute Δ arrangement as determined by the structure refinement is likely the correct determination.

Interestingly, as the structures were solved and checked for validity, it was noted that several of the final solutions had substantial "void" spaces present in the unit cell lattice. The compounds that displayed this behavior were **4**, **4a**, **6**, **7**, **8**, **9a**, **11**, **12**, and **13**. The most visually observed void space was found for **6** (shown Figure 6b) with the remaining packing diagrams available in the Supporting Information. These voids were large enough that the checkCIF analyses indicated additional solvent molecules should be present in the space for each structure. A search of the electron density maps indicates that for these structures, no electron density peaks were present in the voids. Apparently, formation of these unusually large voids is driven by packing influences of

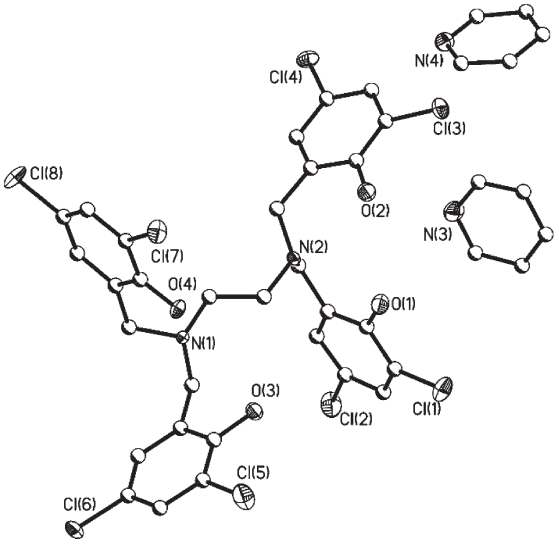

Figure 3. Structure plot of **2**•2py. Heavy atom thermal ellipsoids drawn at 30% level, and carbon atoms drawn as ball and stick for simplicity.

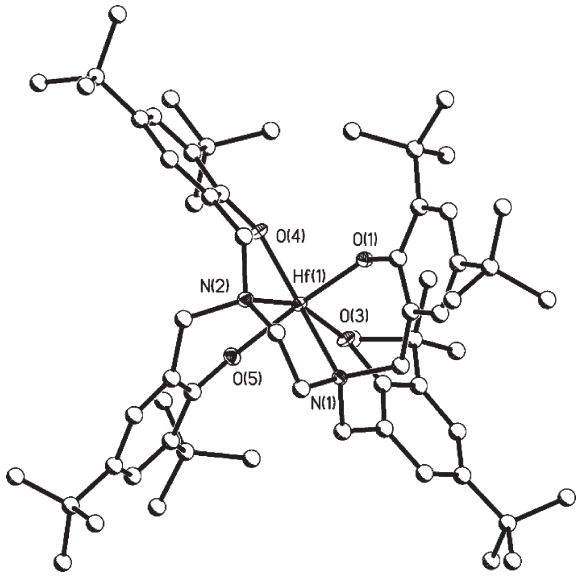

Figure 4. Structure plot of **5**. Heavy atom thermal ellipsoids drawn at 30% level, and carbon atoms drawn as ball and stick for simplicity.

Table 3. Select Averaged Metrical Data for **3**−**13**

comp'd	av M−O (Å) ED-L_4	av M−N (Å) ED-L_4	av O−M−O (deg)	av O−M−N (deg)	av N−M−N (deg)
Ti(ED-Bz_4)•(CH_2Cl_2)[38]	1.88	2.25	94.2, 165.9	85.2, 166.1	80.5
3	1.88	2.25	92.6, 109.5, 170.9	86.3, 163.8	79.1
4	2.01	2.38	93.51, 119.2, 166.2	87.0, 156.6	75.9
4a	2.00	2.38	92.7, 120.0, 166.0	83.9, 156.3	75.4
5	2.00	2.35	93.2, 116.7, 167.6	82.0, 90.3, 158.1	76.4
6	1.88	2.26	93.9, 111.4, 166.0	84.61, 163.8	80.1
7	2.07	2.51	86.3, 103.0, 146.9	75.7, 140.4	71.2
8	1.99	2.39	97.8, 158.9	84.9, 165.3	74.0
9a	2.24	2.53	112.7, 161.1, 78.0	81.0, 107.2	dna[a]
10	1.92	2.14	127.1	97.0	dna[a]
11	2.08	2.50	96.5	83.5, 78.0	155.7
12	1.80 (Ti-ONep)	2.42 (Ti)	96.8, 101.2, 158.49 (Ti)	82.3, 89.5, 172.6 (Ti)	86.8 (Ti)
	1.90 (Ti/Zn ED-L_4)	2.08 (Zn)	121.3 (Zn)	101.4, 114.5 (Zn)	116.7 (Zn)
13	1.98 (Co)	2.19 (Co)	79.8, 111.6, 113.2 (Co)	90.5, 112.1, 134.1, 156.3 (Co)	82.1 (Co)
	1.81 (Li)	2.03 (Li)	91.2 (Li)	110.2, 140.5 (Li)	dna[a] (Li)

[a] dna = data not available.

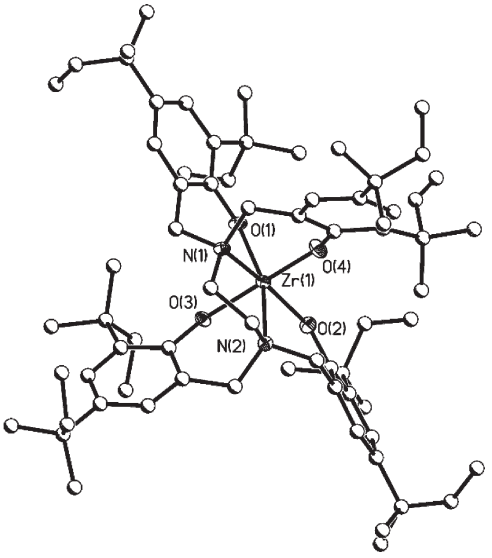

Figure 5. Structure plot of **4a**. Heavy atom thermal ellipsoids drawn at 30% level, and carbon atoms drawn as ball and stick for simplicity.

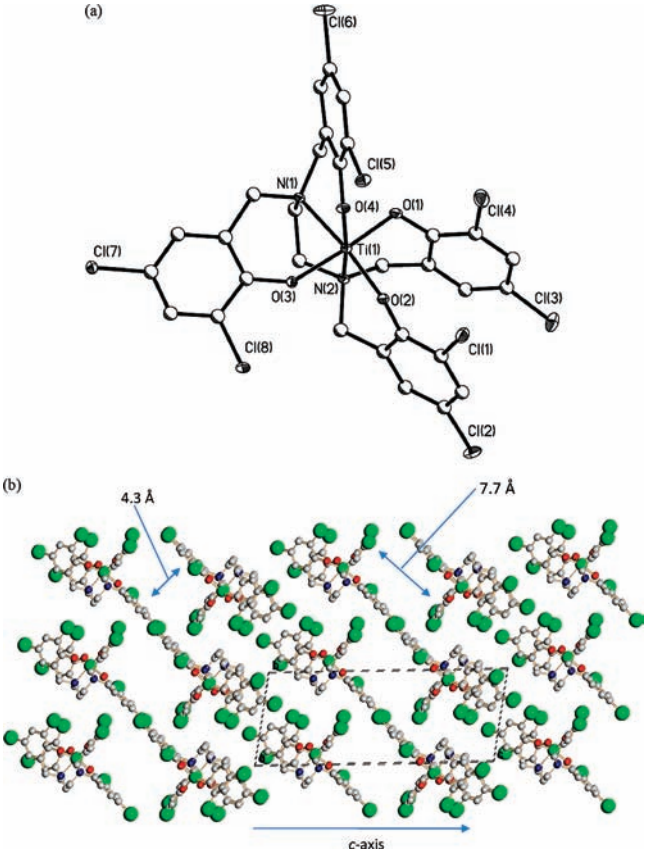

Figure 6. (a) Structure plot of **6**. Heavy atom thermal ellipsoids drawn at 30% level, and carbon atoms drawn as ball and stick for simplicity. (b) Packing diagram for **6** looking down the *a*-axis.

the crystalline molecules themselves and not any significant interactions between the molecules. Analysis of the molecular packing diagrams of those structures with voids reveals only weak H---C interactions at distances considered too long for hydrogen bonding behavior

(48) Gennaro, M. C.; Mirti, P.; Casalino, C. *Polyhedron* **1983**, *2*, 13.

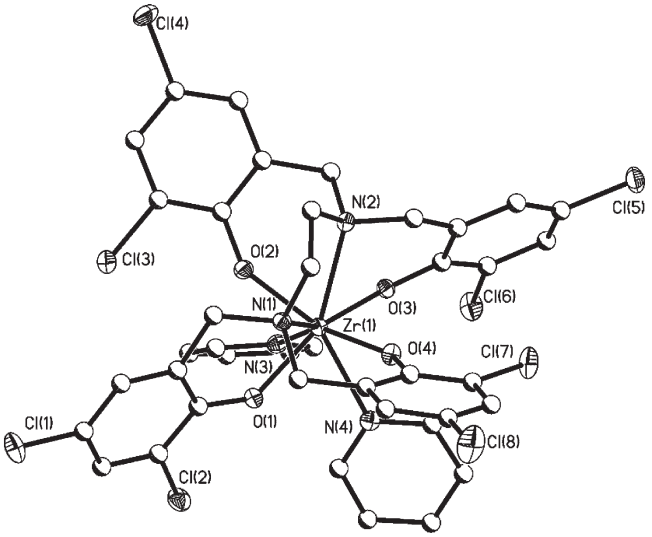

Figure 7. Structure plot of **7**. Heavy atom thermal ellipsoids drawn at 30% level, and carbon atoms drawn as ball and stick for simplicity.

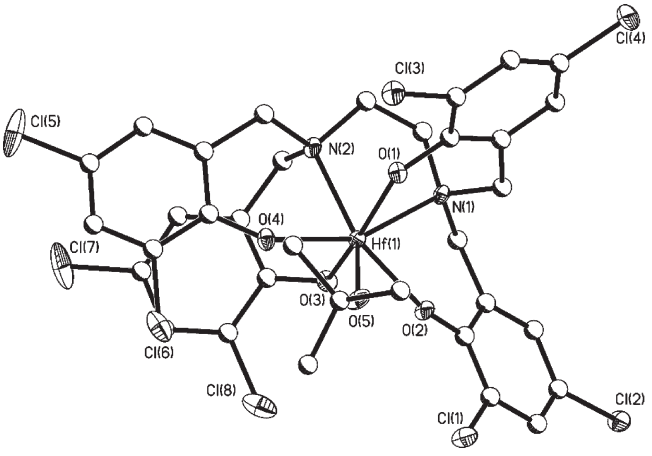

Figure 8. Structure plot of **8**. Heavy atom thermal ellipsoids drawn at 30% level, and carbon atoms drawn as ball and stick for simplicity.

(i.e., > 2.9 Å). Additional work to understand and exploit these voids is underway.

Table 3 lists the metrical data for **3**−**8**. The bond angles indicate a slight distortion from ideal O_h geometry for **3**−**6** mostly induced by the constraints of the ED-L_4 ligands. Compounds **7** and **8** were found to adopt irregular 8- and 7-coordination geometries forming pseudo dodecahedron and pentagonal bipyramidal geometries, respectively, due to coordination of the solvent molecules and the ED-DCP_4 ligand. As can be discerned, the M−O and M−N distances for **3** and **6** are consistent with each other and the literature values observed for Ti(ED-Bz_4)•(CH_2Cl_2).[38] For **4** and **5**, the M−O distances are slightly elongated in comparison to **3** and ED-Bz_4 derivative, which is readily attributed to the increase in cation size to Zr and Hf.[47] The same variation is noted for **7** and **8**; however, the change in coordination and electron donation of the bound solvent may also account for this slight elongation.

Elemental analyses of **3**−**8** were *not* found to be consistent with the solid-state structures. While some of the results reported do appear to agree with the crystal

structure, it is of note that the results varied considerably from each attempt on a particular complex. In fact, on some analyses of these compounds, *negative N* values were recorded. Because of the completely encapsulated species and handling of the samples under argon atmospheres, it is not likely that this variation is a result of sample reaction with exposure to circumambient atmosphere. Presumably, the inconsistencies resulted from the inclusion of solvent (possibly in the voids previously discussed), trace amounts of unreacted ligand as noted in the NMR data for some of the compounds (vide infra), or an unusual decomposition pathway (i.e., M−N formation versus the expected M−O formation). The first two potential complications would not explain the negative *N* values. PXRD of crystals of **3**−**8** under an argon atmosphere up to 600 °C indicated that a variety of phases had formed during processing: **3**−**5**, amorphous; **6**, anatase; **7**, zirconium oxide; **8**, hafnium oxide/nitride. The potential formation of nitrides would obfuscate the final elemental analyses by the combustion process. Further, it was noted during the heating of these materials that some of these compounds preferentially melted as opposed to decomposing. Melting point temperatures were determined for these compounds (**Compound**, MP °C): **3**, 324; **4**, > 360; **5**, 354; **6**, > 360; **7**, 250; **8**, 250 (*note:* the MelTemp had an upper limit of 360 °C). The sharp start/end melting points observed for the majority of these compounds indicates that pure materials were used in this analysis. The formation of a volatile solution phase (as opposed to the standard decomposition) at relatively low temperatures has previously been shown to cause difficulty acquiring elemental analyses on crystalline $M(OR)_4$ materials.[18] Therefore, this physical property combined with the PXRD data indicates that some of these compounds are volatile and/or form mixed nitrogen bearing phases, thus making it difficult to obtain acceptable elemental analyses by the combustion method employed here.

Solution Behavior. NMR studies were therefore explored to investigate the purity of the bulk materials of **3**−**8** and determine their solution behavior in $CDCl_3$. The spectra of **1**, **1a**, and **2** ($CDCl_3$) were in full agreement with the proposed and observed structures, consisting of 5 proton resonances: one hydroxyl singlet (4H), two aryloxide doublets (4H apiece), one benzylic singlet (8H), and one ethylene diamine singlet (4H). In addition, for **1**, two distinct singlets were noted for the two *t*-butyl groups and for **1a**, two sets of amyl resonances were observed. The relatively simple ^{1}H NMR spectra observed are due in part to the internal mirror plane and C_2 axis of the ligands.

It was expected that the NMR spectra of coordinated ligands would be far more complicated than the free-ligand spectra upon complexation.[48] One way to visualize the binding of **1**, **1a**, and **2** is to divide the four phenoxides of **1**, **1a**, or **2** into two groups, one with an in-plane (OAr^{IP}) and one with an out-of-plane (OAr^{OP}) pair where the plane refers to the phenoxy group formed by the metal and the two nitrogen atoms. The two aromatic H's and the two *t*-butyl groups of the phenol rings are therefore split into two distinct environments, effectively doubling the number of peaks expected. The benzylic protons of **1** and **2** have the potential to appear as four unique peaks, resulting from axial and equatorial positioning within the OAr^{IP} and OAr^{OP} pairs. These benzylic peaks can interconvert, and in addition the nitrogen atoms themselves are potentially capable of lone pair inversions.

In toluene-d_8, the ^{1}H NMR spectra obtained of **3**−**8** had multiple overlapping resonances, which made interpretation difficult. Initial attempts to obtain the ^{1}H spectrum of these compounds in $CDCl_3$ yielded greatly simplified spectra that presented six methylene doublets. This suggested that the structure was retained in solution through the generation of diastereotopic methylene protons; however, discrepancies between the expected and calculated integration of the aryl and the methylene protons required additional studies. A series of 2D-NMR studies revealed the presence of "free H_4-ED-R_4 ligand" for each sample of **3**−**8**, which significantly overlap with the complex resonances and lead to inaccurate integration ratios. Furthermore, the amount of free ligand noted for a particular compound, varied from sample to sample. The generation and variability of the free ligand within a given sample was believed to be due to hydrolysis or acidification by the "dry" $CDCl_3$. Dissolution of the same compounds in cyclohexane-d_{12} eliminated this problem while maintaining the simplified spectra.

For **3**, in cyclohexane-d_{12} four aryl singlets, six methylene doublets, and four butyl singlets were observed. In addition, resonances associated with some free H_4-ED-DBP_4 were also observed in the spectrum of **3**, even after multiple recrystallizations. For **4** (see spectrum in the Supporting Information) and **5** three aryl singlets (1:1:2 ratio), six equivalent methylene doublets, and four equivalent butyl singlets in an overall 4:6:36 ratio were recorded. These data indicate that the OAr^{IP} and OAr^{OP} phenoxides are not equivalent with each other generating diastereotopic methylene protons that yields four $[CH_2N\text{-}(CH_2\text{-}DBP)_2]_2$ and two $[CH_2N\text{-}(CH_2\text{-}DBP)_2]_2$ doublets. The reduced number of aryl resonances in these spectra was believed to be due to coincidental overlapping resonances. Therefore it can be concluded that in cyclo-d_{12}, the bulk materials of **3**−**5** were consistent with their respective single crystal structures maintaining a monomeric species and the hexadentate coordination.

For the **1a** derivatives, four aryl singlets and six diastereotopic doublets were expected and observed in an overall 4:6 ratio. Further, because of the amyl substituent $[(CH_3)_2C(CH_2CH_3)]$, there are a two sets of alkyl (singlets, triplets, quartets) resonances observed which overlap and complicate the spectra; however, the overall total peak integration is consistent with the expected 44H value. The presence of free ligand associated with **1a** was noted in the spectrum of **5a**, which complicates the integration. For both **4a** and **5a**, the NMR data indicates that the structures are retained in solution.

Since **2** has no alkyl substituents on the aromatic ring, the spectrum of the chelated species was expected to be simplified. For **6**, the complex was sparingly soluble in cyclo-d_{12} and thus the free solvents employed in the synthesis (toluene and pyridine) dominated the spectrum, yielding little useful information. Dissolution of **2** in py-d_5 revealed that the OAr^{IP} and OAr^{OP} are inequivalent within their pairs showing six doublets of the methylene confirming the purity and structural retention in solution. In comparison, compound **7** was much more soluble in

cyclo-d_{12}, possibly because of the bound pyridine, yielding the standard three pyridine resonances, four aryl protons, four methylene doublets assigned to the aryl methylene protons, and two broad singlets consistent with the ethylene diamine protons, in an overall 4:4:2 ratio. This indicates that the solution state structure of **7** is consistent with the hexadentate ED-R_4 solid-state structure. In contrast, **8** has two aromatic proton singlets, six doublets for the diastereotopic benzyl protons, and a single butyl peak for the bound H-OBu^t that overlaps with the cyclo-d_{12} resonance. The expected 4:6 ratio of aryl/methylene protons is roughly observed which indicates that the aromatic protons are coincidentally overlapping. Again, on the basis of these data it can be concluded that the ligands maintain their complete encapsulation of the cations for **6**−**8** and thus the structures are maintained in solution.

Mass Spectroscopy. Mass spectroscopic analyses are not typically of use for metal alkoxides because of the oligomerization that often occurs in the gas phase. However, with the hexadentate, encapsulated ED-R_4 derivatives isolated in this effort, any oligomerization should be minimized and information pertaining to the identification of these compounds should be possible. Mass spectral analyses of **3**−**7** indicated that $[M+H]^+$ peaks for each compound were consistent with the single crystal structures. For **3**, a significant peak consistent with the free ligand was observed, which was expected based on the NMR data. For **8** the compound was poorly soluble and a meaningful spectrum could not be obtained. However, in general, these data indicate that the bulk material is consistent with their single crystal X-ray structure.

Alternative Cations. Since the group 4 cations were found to accommodate the full charge of the polydentate ED-L_4 species, it was of interest to determine the coordination behavior of lower oxidation state cations with these ligands. Since the literature had already reported the +2 species, as noted for [Zn(ED-DMP$_3$(H-DMP))]-[Na],[35] efforts continued in this vein exploring Ca^{2+}, Zn^{2+}, and Sn^{2+} which were identified as **9a**− **13** by FTIR, single crystal X-ray structure, and NMR spectroscopy when possible.

Using 2 equiv of $Ca(NR_2)_2$, we anticipated the complete substitution of the ED-L_4 ligand for the amides (eq 2). The initial reactions were conducted in tol, whereupon a white precipitate formed which could not be redissolved with heating; however, the addition of THF or py led to the rapid dissolution of the precipitate. X-ray quality crystals were grown by slow evaporation of the volatile component, leading to the isolation of **9a** or **9b** from THF (Figure 9a) or py (Figure 9b), respectively. For **9a** the ED-(DBP)$_4$ ligand was solved as a symmetrical dinuclear species wherein, the "N(CH$_2$)$_2$N" moiety also acts as a bridge to connect each trigonal bipyramidal (tbp) Ca metal center. Each half of the ethylene diamine ligand binds to a Ca metal center using one DBP one μ-DBP, the parent N, and a THF molecule.

$$\underset{(1)}{2Ca(NR_2)_2} + \underset{}{H_4\text{-ED-DBP}_4} \rightarrow \underset{(9)}{\text{'}Ca_2(\text{ED-DBP}_4)'} \quad (2)$$

In contrast, when isolated from py the same empirical moiety Ca_2(ED-DBP$_4$)(solv) (**9b**, see Figure 9c) was isolated however, in a substantially different arrangement as determined by single crystal X-ray diffraction studies. It is of note that the structural solution of **9b** was not of high enough quality to allow for final refinement but the connectivity was unequivocally established (the unit cell data is presented in Table 2 to assist in its identification). For **9b**, the polymer consists of alternating solvated and non-solvated metal centers adopting either tetrahedral (T_d) or distorted trigonal planar geometries. The py solvent molecules bind to the polymer on the opposite side of the ED-DBP$_4$ moieties. The Ca centers only use the O atoms of the same ED-DBP$_4$ moiety with no coordination sites filled by the N atoms to form a [−Ca−(μ-O)−Ca′−(μ-O′)−]$_2$ subunit chain. The site was expected to be occupied by the N binding but instead is filled by the π-interaction of the aryl ring of the DBP moiety to the next Ca atom. The chain is propagated by the bridging of the final DBP ligand of the first subunit to the first Ca of the second subunit through the oxygen atom. Again, an η-interaction of the DBP to the second Ca of the second subunit occurs. This forces the second ED-DBP$_4$ ligand to be *trans* to the original one, leading a screw axis of the ED-DBP$_4$ ligand around the Ca−O−Ca chain. The NMR spectrum of **9b** in py-d_5 appears to generate a symmetric compound with broad methylene resonances. This may be due to rapid exchange of the py ligands and with dynamic binding of the ED-DBP$_4$

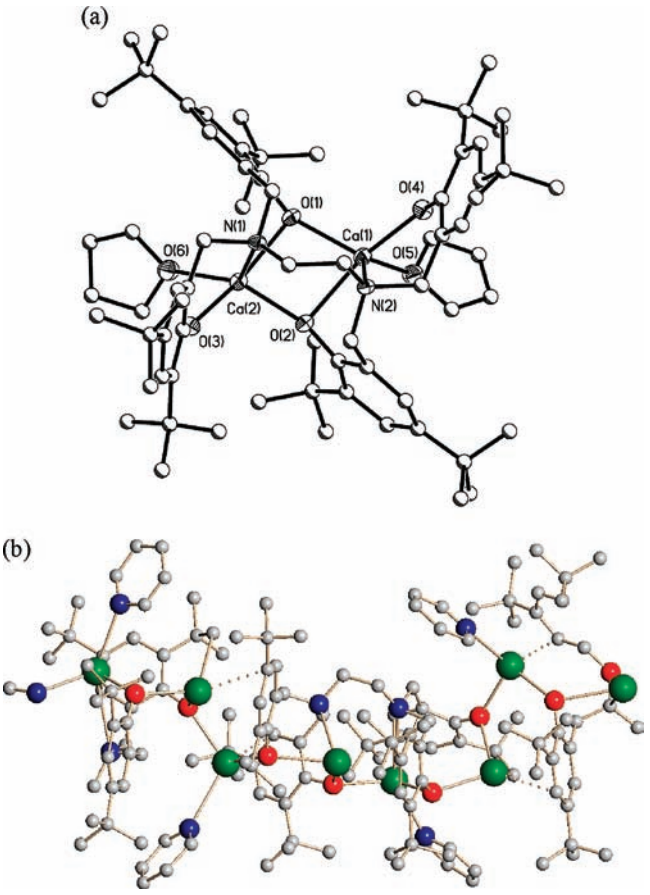

Figure 9. (a) Structure plot of **9a**. Heavy atom thermal ellipsoids drawn at 30% level and carbon atoms drawn as ball and stick for simplicity. (b) Structure plot of **9b**. Since the structural refinement was not possible, the structure is shown in ball stick form (green Ca, blue N, red O, and gray C; H not shown for clarity).

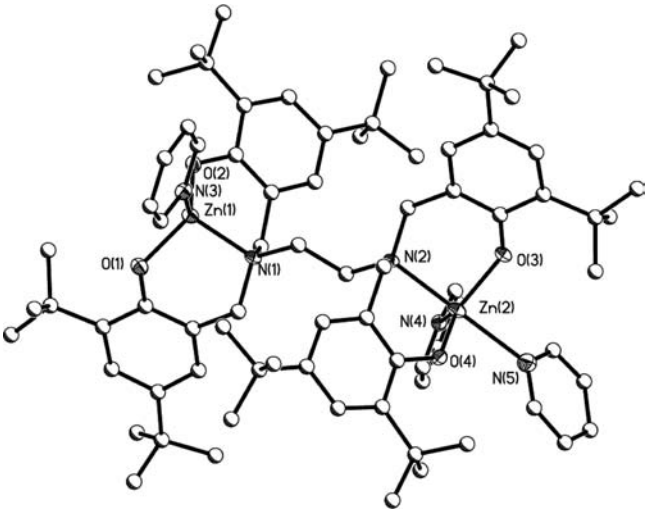

Figure 10. Structure plot of **10**. Heavy atom thermal ellipsoids drawn at 30% level, and carbon atoms drawn as ball and stick for simplicity.

ligand. These broad peaks limit the information that can be deduced pertaining to the solution structure of **9b**.

It was of interest to contrast the coordination behavior of the +2 alkaline earth to the late transition metal cations. As mentioned previously, the [Zn(ED-DMP$_3$-(H-DMP))][Na][35] salt complex was found to be monomeric with a tbp geometry and one of the OH not reacted but the use of $ZnEt_2$ was expected to lead to a different coordination geometry. The reaction of 2 equiv of $ZnEt_2$ with **1** (eq 3) formed a precipitate, which was easily dissolved upon addition of py. The resulting crystals proved to be **10** (Figure 10) •5py. Again, a dinuclear complex was isolated but instead of any interaction between the Zn metal centers, the two cations are bridged only by the "$N(CH_2)_2N$". The Zn cations each bind two phenoxides and the N from the parent moiety but yield different coordination geometries of T_d and tbp based upon the coordination of one or two py solvent molecules, respectively. Five py solvent molecules were located in the unit cell lattice. The NMR spectrum of **10** reveals three py, two aryl, a set of broad methylene singlets, and two butyl resonances. This is consistent with the D_{2d} symmetry of the solid-state structure if equal numbers of py are bound to the Zn metal center, which would be expected upon dissolution in py-d_5. The rapid exchange of the py ligands most likely contributes to the broadened methylene peaks.

$$\underset{(1)}{2ZnEt_2 + H_4\text{-ED-DBP}_4} \rightarrow \underset{(10)}{[(py)Zn][\mu\text{-ED-(DBP)}_4][Zn(py)_2]} \quad (3)$$

Altering the cation to the main group Sn^{2+} cation yielded **11** (Figure 11) from the exchange of $Sn(NMe_2)_2$ with **1** in tol followed by subsequent addition of py. In contrast to **10**, the structure of **11** is symmetric where the Sn^{2+} metal centers were found to be T_d bound by two phenoxy O atoms, the parent N atom, and one py solvent molecule. The NMR spectrum of **11**was consistent with the D_{2d} symmetry expected from the solid-state structure with a singlet for the two aryl protons, three doublets for

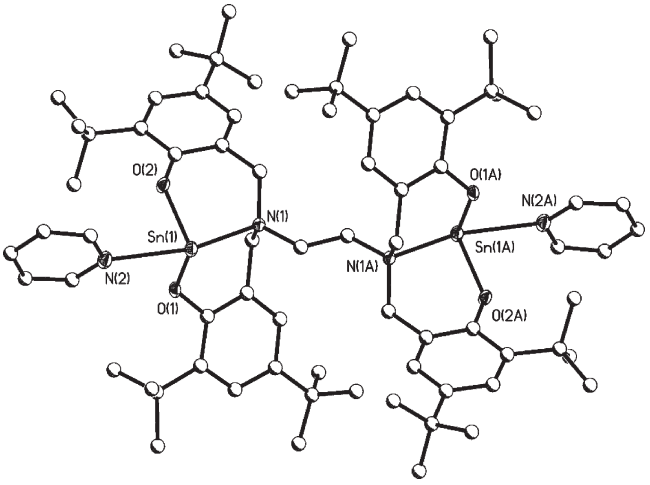

Figure 11. Structure plot of **11**. Heavy atom thermal ellipsoids drawn at 30% level, and carbon atoms drawn as ball and stick for simplicity.

the diasterotopic methylene protons, and two singlets for the butyl groups.

$$\underset{(1)}{2Sn(N(SiMe_3)_2)_2 + H_4\text{-ED-DBP}_4} \rightarrow \underset{(11)}{[(py)Sn]_2(\text{ED-DBP}_4)} \quad (4)$$

An attempt to generate mixed cationic compounds was undertaken using $ZnEt_2$ followed by addition of $[Ti(ONep)_4]_2$ (eq 5). The successful stepwise exchange led to the isolation of **12** (Figure 12). The two metals do not interact but individually bind to **1** through the two O atoms of the DBP and the parent N atom. This leaves two ONep ligands bound to the Ti metal center. Both the Ti and Zn metal centers finish their O_h and T_d coordination, respectively, by binding a py solvent molecule. The NMR spectrum of **12** was extremely complicated because of overlapping resonances, and exact information pertaining to the solution behavior of **12** was not possible; however, doublets for the diastereotopic protons of the ED-DBP ligand, along with ONep methylene and methyl resonances were observed, implying retention of the overall structure.

$$\underset{(1)}{ZnEt_2 + H_4\text{-ED-L}_4} \xrightarrow{+Ti(ONep)_4} \underset{(12)}{(py)(ONep)_2\,Ti(\text{ED-DBP}_4)Zn(py)} \quad (5)$$

Because of the success with sequential substitution, an investigation of the single source double alkoxide Co-$[\mu\text{-OC}_6H_4(CHMe_2)_2\text{-}2)_2Li(py)_2]_2$[12] with H_4-ED-DBP$_4$ was undertaken (eq 6). The reaction proceeded with no color change (maintained the initial purple color), which is consistent with a Co^{2+} charge metal center. Interestingly, the original dimer is disrupted to form **13** (Figure 13) wherein the Co was solved in a square base pyramidal (sbp) geometry using two N and three O atoms of the ED-DBP$_4$ ligand. Two of the O atoms bind to the Li, which also has a solvent of py bound to complete its trigonal planar geometry. On the basis of charge balance, this indicates that a proton should remain on one of the DBP moieties. This was located in the electron density map and resides on one of the phenoxide rings that points

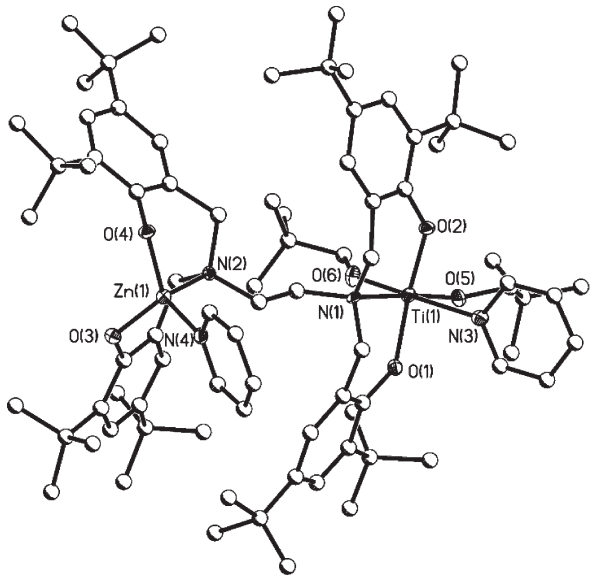

Figure 12. Structure plot of **12**. Heavy atom thermal ellipsoids drawn at 30% level, and carbon atoms drawn as ball and stick for simplicity.

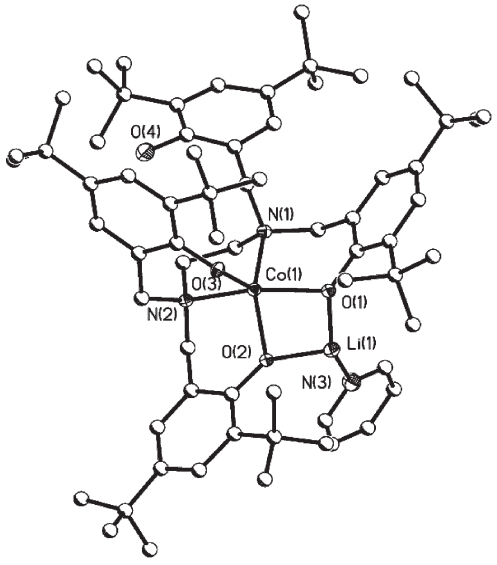

Figure 13. Structure plot of **13**. Heavy atom thermal ellipsoids drawn at 30% level, and carbon atoms drawn as ball and stick for simplicity.

away from the Co metal. NMR data did not prove useful in identification of the bulk powder because of the paramagnetic Co^{2+} metal center.

$$\underset{(1)}{Co[\mu\text{-}OC_6H_4(CHMe_2)_2\text{-}2)_2Li(py)_2]_2} + \underset{}{H_4\text{-ED-DBP}_4} \rightarrow \underset{(13)}{(py)Li[ED\text{-}DBP_3(H\text{-}DBP)]Co} \quad (6)$$

Because of the variable elemental analyses recorded for the simple homometallic species (**3**−**8**) due to unusual decomposition pathways, it was not expected that the complex cationic species (**9**− **13**) would be amenable to similar analyses. Further, these species all possessed bound solvent molecules which often complicates the final analyses because of premature loss at elevated temperatures. Therefore, it was not surprising that the complex heterometallic complexes also exhibited inaccurate analyses. Further, the mass spectral analyses of **10** and **11** revealed mainly free ligand which was expected because of the open nature of the compounds and the high volatility of the metals.

The metrical data for the alternative metals (**9a**−**13**) are collected in Table 3. The cation size of Ca (1.14 Å, 6 coordination) is significantly larger in comparison to Ti (0.745 Å), and this explains the significantly longer M−O and M−N distances noted for **9a**. The T_d geometry noted in **9b** is unusual with only seven $Ca(OR)_2(L)_2$ compounds previously characterized with this reduced geometry.[49−55] Only one of those was an alkoxide identified as $[(THF)(OR)Ca(\mu\text{-}OR)]_2$ where OR = $OC(C_6H_5)_2CH_2\text{-}(C_6H_4Cl\text{-}4)_2$.[49] In contrast, the M−O and M−N distances of **10** are longer and shorter for Zn (0.74 Å) in comparison to those of **3**, even with similar sized cations. This trend was also noted for **12**, which has py bound to an O_h-bound Ti and T_d-bound Zn metal centers. The sbp Co (0.92 Å) and T_d Li (0.90 Å) in **13** were solved with different distances because of the unusual binding of the ED-DBP_4 ligand.

Conclusion

The investigation of the coordination behavior of the polydentate ED-L_4 (**1**, R = DBP; **1a** = DAP, **2** R = DCP) ligands has led to the development of a novel family of compounds with complex coordination directed by the metal cations and the substituents on the pendant rings. The group 4 species yielded completely encapsulated species crystallographically characterized as M(ED-DBP_4), **3**−**5a** and M(ED-DCP_4) (**6**). Surprisingly, additional solvent ligands were found bound to the metals of the ED-DCP_4 derivatives **7** and **8**. This was attributed to the large cation size and the induced electronic effect based on the ring substitutents (Cl vs Bu^t). Solution NMR reveals that the symmetry of the parent ligands (**1**, **1a**, and **2**) was destroyed upon complexation to the metals, but the monomeric nature of the compounds was maintained in cyclohexane-d_{12}. Lower oxidation state cations (alkaline earth, late transition metal, and main group) were found to bind with **1** forming dinuclear (**9a**, **10** and **11**) and polymeric (**9b**) species. Furthermore, mixed metal ED-DBP_4 compounds (**12** and **13**) were also isolable from sequential addition or single source precursor reactions. Combined these efforts demonstrate the complex coordination behavior and utility of the ED-L_4 ligands in terms of producing controlled structured M-$(OR)_x$. It is expected that further development of these types of ligands will facilitate controlled construction of even more complex $M(OR)_x$ for ceramic materials applications.

(49) Tesh, K. F.; Hanusa, T. P.; Huffman, J. C.; Huffman, C. J. *Inorg. Chem.* **1992**, *31*, 5572.
(50) Westerhausen, M.; Hartmann, M.; Makropoulus, N.; Wieneke, B.; Schwartz, W.; Stalke, D. *Z. Naturforsch. B. Chem. Sci.* **1998**, *53*, 117.
(51) Cloke, F. G. N.; Hitchock, P. B.; Lappert, M. F.; Lawless, G. A.; Royo, B. *J. Chem. Soc., Chem. Commun.* **1991**, 724.
(52) Varga, W.; Englich, U.; Ruhlandt-Senge, K. *Inorg. Chem.* **2002**, *41*, 5602.
(53) Westerhausen, M.; Schwarz, W. *Z. Anorg. Allg. Chem.* **1991**, *606*, 177.
(54) He, X. Y.; Noll, B. C.; Beatty, A.; Mulvey, R. E.; Henderson, K. W. *J. Am. Chem. Soc.* **2004**, *126*, 7444.
(55) Tang, Y. J.; Zaqkharov, L. N.; Kassel, W. S.; Rheingold, A. L.; Kemp, R. A. *Inorg. Chim. Acta* **2005**, *258*, 2014.

Acknowledgment. The authors would like to thank Ms. C. Higham, Mr. Niconchuk, and Ms. B. Bergeron (College of Holy Cross) and Ms. T. Doan (AIMS@UNM High School) for technical synthetic assistance, and UMass Amherst Mass Spectrometry Center for assistance with all high resolution MS data. For support of this research, the authors thank the Research Corporation for a Cottrell College Science Award (CC6827) and the U.S. Department of Energy, Office of Basic Energy Science, Division of Material Sciences and Engineering. Sandia is a multiprogram laboratory operated by Sandia Corporation, a Lockheed Martin Company, for the United States Department of Energy's National Nuclear Security Administration under contract DE-AC04-94AL85000.

Supporting Information Available: Additional information as noted in the text. This material is available free of charge via the Internet at http://pubs.acs.org. The crystal structures for **1**−**13** have been deposited at the Cambridge Crystallographic Data Centre and allocated the deposition nos. CCDC 727272−727285. These data can be obtained free of charge via http://www.ccdc.cam.ac.uk/conts/retrieving.html, or from the Cambridge Crystallographic Data Centre, 12 Union Road, Cambridge CB2 1EZ, U.K.; fax: (44) 01223−336033; or e-mail: deposit@ccdc.cam.ac.uk.